OPTIMIZATION OF WELD BEAD GEOMETRIC PARAMETERS IN A TIG WELDING PROCESS

A Thesis Submitted to
The Graduate School of Engineering and Science of
İzmir Institute of Technology
in Partial Fulfillment of the Requirements for the Degree of

MASTER OF SCIENCE

in Mechanical Engineering

by

Kadriye Çağla DİLSİZ

July 2019
İZMİR

We approve the thesis of **Kadriye Çağla DİLSİZ**

Examining Committee Members:

Assoc. Prof. Dr. H. Seçil ARTEM
Department of Mechanical Engineering, İzmir Institute of Technology

Assist. Prof. Dr. Ebubekir ATAN
Department of Mechanical Engineering, İzmir Katip Çelebi University

Assist. Prof. Dr. Kasım TOPRAK
Department of Mechanical Engineering, İzmir Institute of Technology

17 July 2019

Assoc. Prof. Dr. H. Seçil ARTEM
Supervisor, Department of Mechanical Engineering, İzmir Institute of Technology

Prof. Dr. Sedat AKKURT
Head of the Department of Mechanical Engineering

Prof. Dr. Aysun SOFUOĞLU
Dean of the Graduate School of Engineering and Science

ACKNOWLEDGMENTS

I would like to express my profound thanks to my supervisor Assoc. Prof. Dr. H. Seçil Artem for her patience, guidance, kindness, support and endless encouragement. Her vision, sincerity, and motivation have deeply inspired me.

I would like to thank also Assist. Prof. Dr. Levent Aydın who helped me with his valuable suggestions and guidance has been helpful in every phases of the completion of my study.

I am extremely grateful to my family for their love, prayers, caring, and preparing me for my future. I am very much thankful to my mother for her understanding, and continuing support.

I would like to thank my precious friends Bahadır Öztürk and Merve Özkahya for their encouragement, support, and motivation.

Lastly, I am very thankful to my beloved friend Arda Özkan for his love, caring, support, and motivation.

ABSTRACT

OPTIMIZATION OF WELD BEAD GEOMETRIC PARAMETERS IN A TIG WELDING PROCESS

Welding is a process that widely used in many areas of industry. Tungsten Inert Gas (TIG) welding process in several types of welding is often preferred in space and aircraft industry, defense industry, and automotive. The welding should be at the required limits and quality when working under pressure. Visual and physical welding quality determined by welding bead geometric parameters. Weld bead dimensions response variables as front height (FH), front width (FW), back height (BH), and back width (BW). In this thesis, Neuro-regression approach which is hybrid study of conventional regression analysis and artificial neural network. Third order polynomial function is used to design front width response itself. The differences between neuro-regression approach and conventional regression analysis while modeling the weld bead geometric dimensions are examined. Welding speed, wire feed rate, percentage of cleaning, gap, and welding current are taken as input variables of the system during modeling. Effects of welding speed, wire feed rate, percentage of cleaning, gap, and welding current on front height, front width, back height, and back width are expressed. Optimization of weld bead geometric parameters in TIG welding process were carried out by using Differential Evolution, Nelder Mead, Simulated Annealing and Random Search stochastic optimization algorithms. Two different problems of front width are studied. Differential Evolution is selected as stochastic search method to have minimum value of front width as a result of the study. All mathematical calculations are carried in Wolfram Mathematica.

ÖZET

TIG KAYNAĞI İŞLEMİNDEKİ KAYNAK DİKİŞİ GEOMETRİK PARAMETRELERİNİN OPTİMİZASYONU

Kaynak endüstrinin bir çok alanında yaygın olarak kullanılan bir prosestir. Bir çok kaynak türünün içinde TIG kaynağı uzay ve uçak sanayi, savunma sanayi, ve otomotiv alanlarında sıkça tercih edilir. Kaynağın basınç altında çalışacağı durumlarda istenilen limitlerde ve kalitede olması gerekmektedir. Kaynak kalitesini görsel ve fiziksel olarak kaynak dikişi ölçüleri belirler. Kaynak dikişinin kesit geometrisi üst yükseklik (FH), üst genişlik (FW), alt yükseklik (BH) ve alt genişlik (BW) ölçülerinden oluşur. Bu tezde Nöro-regresyon yaklaşımı kullanılmıştır. Nöro-regresyon yaklaşımı, geleneksel regresyon analizi ve yapay sinir ağları kullanımının hibrit bir çalışmasıdır. Üst genişlik 3. dereceden bir polinom ile ifade edilmiştir. Nöro-regresyon ve geleneksel regresyon ile yapılan çalışmaşalarda üst genişliğin modellemesi esnasında karşılaşılan R^2 sonuçları karşılaştırılmıştır. Kaynak hızı, kaynak besleme oranı, temizlik yüzdesi, boşluk ve kaynak akımı parametreleri bu çalışmada model girdisi olarak alınmıştır. Diferansiyel Gelişim, Değiştirilmiş Nelder Mead, Benzetilmiş Tavlama ve Rastgele Arama stokastik optimizasyon algoritmaları kulllanılarak kaynak dikişine ait ölçülerin optimizasyonları gerçekleştirilmiştir. Üst genişlik ile ilgili iki ayrı problem çalışılmıştır. Çalışmanın sonucunda Diferansiyel Gelişim metodu, stokastik optimizasyon metodu olarak seçilmiştir. Bütün çalışmalar Wolfram Mathematica programında gerçekleştirilmiştir.

TABLE OF CONTENTS

LIST OF FIGURES

LIST OF TABLES

CHAPTHER 1

INTRODUCTION

1.1. Literature Survey

Welding is very old method, which is widely used to joint structural components. Heat and pressure are crucial elements for quality of weld bead in many kind of welding process. Submerged arc welding, submerged metal arc welding and gas metal arc welding are some of the mostly used welding types that defined by American Welding Society. Arc welding could be defined as process what melts metal and joints components by using electric arc. Gas tungsten arc welding is a welding process, which is using non-consumable tungsten electrode to melt metal and creating weld bead to joint elements together in inert gas as a shielding factor manually or automatically. Commonly direct current is preferred because of the fact that tungsten electrodes attach negative polarity. Alternative current is used to achieve different applications and results in some cases. Argon and helium are two different kind of gas what are selected in gas tungsten arc welding for various metals with required penetration (Singh, 2016; Choudhary et al., 2018).

Quality of the welding is significant characteristic of manufacturing fields that is subject to control in many areas of industries. One of the welding parameters what affects quality of the welding is geometric dimensions of weld bead. Nanda et al. (2011) examined geometric parameters of weld bead and stated the importance of these parameters as an affecting element to quality of welding. Welding process could be expressed and modeled with mathematical statements as lots of processes that have well defined inputs and outputs. Welding, which is willed the best state of itself by doing experiments, modeling and using optimization tools, is became a subject for great numbers of studies. Yang et al. (1993) has study what models submerged arc welding process by using nonlinear regression analysis. Relationship concerning weld bead height, penetration, melting ratio, fusion area, and weld pool is observed using deviation between predicted data and actual data. Starling et al. (1993) designed a linear regression model with input variables as welding current, travel speed, gap width, mean bead height and arc deflection current in gas tungsten arc welding process. These variables are selected by implementing design of experiment study. Bead shape is defined as an objective of the study. Result of the application showed that magnetic arc oscillation has positive effect on bead shape. Koleva (2001) considered electron beam power, welding velocity, distance from main surface of magnetic lens of the gun to the focus of the electron beam, and the distance between magnetic lens and the surface of the sample are considered as input variables in electron beam welding process with material stainless steel. The aim is to have depth and width of the weld as objectives. Second order polynomial regression models are generated for both depth and height of the weld.

Shao et al. (2017) investigated gas metal arc welding parameters. Welding current, welding voltage, and welding speed is modeled by implementing finite element method with the material low-carbon steel. Data is collected with design of experiments. Final model is designed by using polynomial regression that is optimized with multi-objective optimization method and compared with multi-objective particle swarm optimization. Vedrtnam et al. (2018) studied to optimize submerged arc welding on stainless steel taking inputs within welding process parameters, which are arc voltage, welding current, nozzle to plate distance, and welding speed. Input parameters, which are modeled implementing response surface methodology (RSM) is optimized for qualified weld bead. Choudhary et al. (2018) conducted an optimization study with inputs, which are voltage, wire feed rate, welding speed, flux condition, and plate thickness. Genetic algorithm, Jaya algorithm, and desirability approach are used in this examination of submerged arc welding. Bead parameters as width, reinforcement, and penetration were used the design by implementing multiple linear regression analysis. Dolas and Bodkhe (2018) aimed to raise depth of penetration in tungsten inert gas (TIG) welding process with material as stainless steel alloy. Linear regression model is generated with inputs that are welding current, welding speed, and gap. ANOVA is adapted to understand influence of inputs to the result. It is seen that welding current has major effect on depth of penetration. Response surface methodology is used to optimize linear regression model. Murugan et al. (2005) carried an optimization study in submerged arc welding process for surface applications. Arc voltage, wire feed rate rate, welding speed, and nozzle-to-plate distance were variables to control process. Analysis of variance is applied to understand corresponding final designs. Lee et al. (2000) studied with multiple regression analysis back to forward and forward to back which takes welding process as an input with weld bead dimension output, and opposite of taking process parameters and dimensions as inputs and outputs.

Tarng and Yang (1998) applied Taguchi method to gas tungsten arc welding process. Artificial neural network is operated to design by using front width, front height, back width, and back height of weld bead geometry. Dutta et al. (2007) modeled gas tungsten arc welding process through the method implementation of linear regression analysis, genetic algorithm, and neural network study. Chan et al. (1999) studied ANN in gas metal arc welding process to model weld geometry. The effects of independent variables, which are arc current, voltage and travel speed on bead width, bead height, penetration, bay angle, and bay length are examined to have optimum results. Problem is reversed and forward model results are compared with base model in addition to study. Tafarroj and Kolahan (2018) studied on polynomial regression model and ANN. In this study, four welding parameters are selected as input variables that are welding voltage, welding speed, welding current and gap. The aim of the study is to define heat source parameters in Goldak heat source model. Destruction is reduced in measurement for parameters of weld pool as a result of application. Wei et al. (2016) applied Fitness Sharing Genetic Algorithm to optimize shielded metal arc weld process. The main objective in the application is to increase energy reduction and thermal efficiency. Welding current and welding velocity are considered as input variables to have objectives. Anderson et al. (1990) explained close relationship between results of artificial neural network and conventional control system for arc welding modeling. Dey at al. (2010) applied welding process to aluminum plates using electron beam. Genetic algorithm is used to minimize welding area dimensions in this application. Welding area is minimized with maximum condition of penetration. Anaca and Olabil (2008) applied Taguchi method to optimize tensile strength in laser welding process. Welding power, welding speed, and focus point position parameters are selected as independent variables in model design. Joby et al. (2015) conducted regression analysis with method of response surface. Tensile strength is examined to defined quality of weld bead. Genetic algorithm and simulated annealing method are applied to have ideal welding parameters. Nagaraju et al. (2016) carried optimization application with a method of genetic algorithm to demonstrate transition between welding current and penetration. Chandrasekhar et al.

(2017) utilized genetic algorithm to maximize the depth of penetration in hybrid laser - tungsten inert gas welding process. Juang and Tarng (2002) examined input variables which are need to be selected to optimize weld bead geometry in TIG welding process with material stainless steel. Arc gap, flow rate, welding current, and welding speed are chosen as independent process input to optimize front height, front width, back height, and back width. Taguchi method is used to reach optimum results.

1.2. Aim of the Study

In the present study, a TIG welding process is modeled by using neuro-regression approach (which is combination of regression modelling and ANN idea) with input variables as welding speed, wire feed rate, percentage of cleaning, gap, and welding current. Four response variables of weld bead geometry which are front height, front width, back height, and back width were modelled. Optimization study is performed to minimize front height by using Differential Evolution (DE), Nelder Mead (NM), Simulated Annealing (SA), and Random Search (RS) stochastic methods in Mathematica software. The steps of thesis study is schematically represented in Figure 1.1.

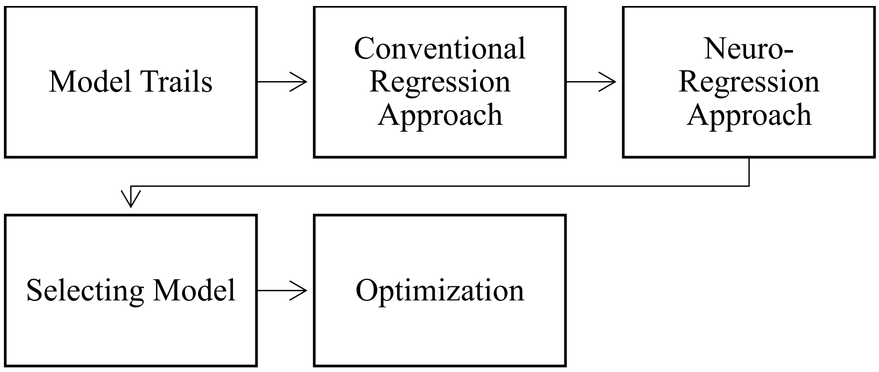

Figure 1.1 Flowchart of thesis study

The main objectives of the thesis are as follows:

- Investigating minimum front height of weld bead geometry,
- Monitoring the effects of independent input variables on each response variables,
- Comparing the result of stochastic search methods; DE, NM, SM, RS.

CHAPTER 2

TIG WELDING

2.1. TIG Welding

Welding is to join between two or more metal pieces by using heat, pressure or both of them together as a general definition. It is divided in to two class as heat welding that uses heat to weld and pressure welding that uses pressure to weld. Heat welding is more commonly preferred nowadays.

During the time before World War I, resistance welding, gas welding, and arc welding are developed which are basic welding process. Arc welding was applied by using carbon electrode shown in Figure 2.1. Afterwards metal rods were begin to use. However, welding area was affected by air and did not have any cover. It was decreased quality of welding. The coated electrode was found by The Swede Oscar Kjellberg. These coated electrodes have increased quality welding.

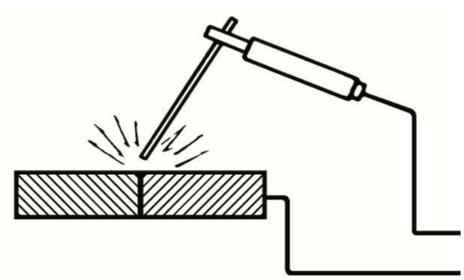

Figure 2.1 Manual Metal Arc Welding

(Source: Weman, 2012)

New methods are developed during 1930s. Continuous wires are used to bring new perspective to welding process to automate the process which was applied manually (Weman, 2012). TIG welding as known as Heliarc Tungsten Gas Welding process was discovered during World War II as a result of methods of combining some of the magnesium and aluminum by American Aerospace Industry. At the end 1930s, tungsten electrode and helium gas were accomplished as a first TIG welding attempting for magnesium welding by Russel Meredith. Heliarc welding has been phenomenon today by collecting details and changing names in the course of time. Argon is used as inert gas in TIG welding in modern day as shown in Figure 2.2 (Ericsson, 2003).

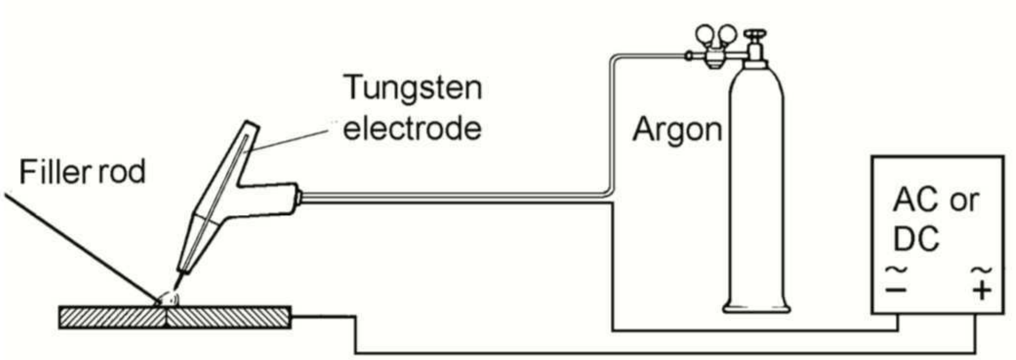

Figure 2.2 TIG Welding Equipment
(Source: Weman, 2012)

Arc welding is extremely complex application using very high temperatures. This application makes the material distorted. It also makes the welding seam open to be cracked, linear indicated and similar kind of failures (Awang, 2002). TIG welding as now as Gas Tungsten Arc welding which is a kind of heat welding is mostly used and very important operation in many of manufacturing areas and applications like vehicles, engines, structures and turbines to name but a few. Heat is used to melt the metal and form a welding seam. To produce this heat, continues electric current is needed that provides an electric arc (Figure 2.3). The main reason of common TIG welding usage is stable arc and easy control of weld seam. Stainless steel, aluminum and magnesium alloys, and copper weldings are significant practice of TIG welding. All the joint types and all welding positions are suitable for TIG welding usage (Weman, 2012).

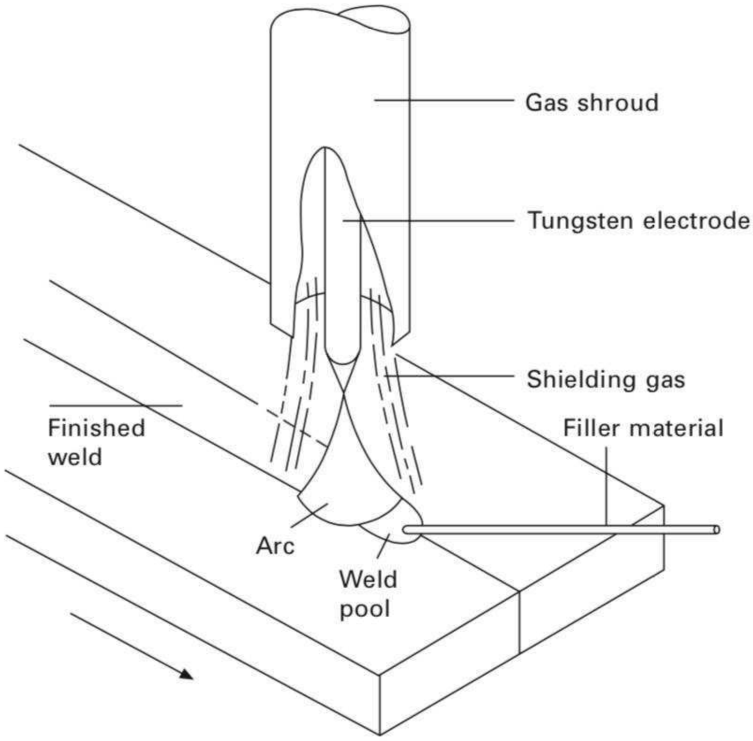

Figure 2.3 TIG welding process

(Source: Norrish, 2006)

The equipment used in TIG welding process are automatic or manual redirect torch, power source, proper inert gas that is under pressure and stocked in containers, and cables. There are two fundamental kinds of torches which are manual that is using manpower and automatic that is machine power. The torch transports exhaustless tungsten electrode and different ceramic nozzles are used for steering to gas stream. Torches are made small-scale, lighter and effortless to use by contrivance of modern plastics and rubbers. It is a great advantage to use slight torch for manual TIG welding. Because manual TIG welding is all about manipulative skills. Nevertheless, capacity of torches should be first priority to select. It is necessary to use a torch that can transfer maximum welding current and welding area should be able to reach by electrode and nozzle. Ordinarily, it is suggested to weld straight down to provide maximum benefit of gravity force. Especially, it is valid for applications that use extra metal as weld wire (Muncaster, 1991).

DC is used for TIG welding in general usage by attaching electrodes in negative way that helps almost all of the heat to influence. Oxide overlay can be broken nothing but positive connection of electrode is available in welding of aluminum. This is the cause of extreme high temperature for electrode. AC is used to avoid all the disadvantages in aluminum and magnesium welding (Weman, 2012).

There are plenty of liquid gases and gas mixtures that can be used in TIG welding which are stocked in pressured tanks. Low temperature is the main influx to hold these gases in liquid form (Muncaster, 1991). These gases could be divided as four groups while examining the process of materials as Weman defined in 2012. However, in this study shielding inert gases are explained for three different metals.

It is very important that to use root gas like argon in welding of stainless steel. Argon is preferred in alloyed steels and low alloyed steels too. It is also generally used in automatic welding. Helium or hydrogen could be added to enhance heat influx with argon. Hydrogen makes the weld tackles and diminishes oxide formation. The single handicap that hydrogen usage has that it can be only used for austenitic stainless steel.

Argon is used as shielding inert gas in welding of aluminum and its alloys. Helium increases heat influx and makes to weld easier for thick metal sheets just as hydrogen. Because of heat increase advantage, in aluminum welding, adding helium to argon is largely operated. Pure helium can be also used in aluminum welding in some circumstances. Arc is narrowed by using helium to increase arc voltage and penetration. Nevertheless, arc stability is reduced and ignition of arc could be more difficult with this increase. Therefore, the automatic welding is mostly done with helium, besides argon is substituent in Manuel welding (Mathers, 2012).

Titanium welding requires majorly high temperature and very good gas purity. Gas purity is expected to be 99.99% or above. Extra protective gas is often used. Because of high shielding performance and density, argon is used. Nevertheless, consisting of more heat, pure helium should be preferred.

Current return cable is the only unbound cable used in TIG welding. This cable must be selected so as not to be affected by the temperature difference. Natural or synthetic rubber covered cable is good choice to use in this TIG welding process. PVC and other covered cables may not have sufficient flexibility in cold weather conditions. Rubber covered cable is the most resistant to heat damage.

Due to work shoes of welders, vehicles on manufacturing area and heavy external factors, these cables should be kept clean and free from damage. The connectors on both ends of the cable must be tight. The cable used should not operate in a loose statement (Muncaster, 1991). Equipment used in TIG welding are presented in Figure 2.4.

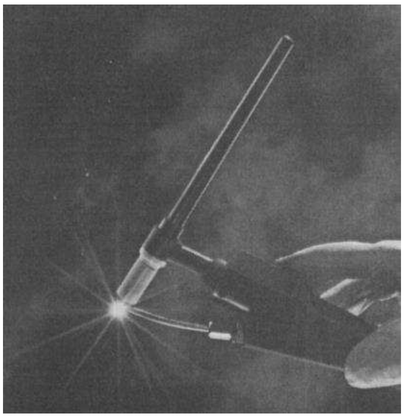

(a)

(b)

(c)

Figure 2.4 TIG Welding Equipment (a) Torch (b) DC (c) Cable
(Source: Muncaster, 1991; Direct Industry; Bob the Welder)

2.2. Advantages and Disadvantages

TIG welding is preferred in several area of industry. It has many advantages and some of disadvantages.

The main advantages of the TIG welding are as follows:

- Welding capability with high quality and less distortion,
- Operating with or without welding wire,
- Suitable with all joint types and all position,
- Proper for thin metal sheets,
- Proper to weld different type of materials,
- Visible arc and welding seam.

The main disadvantages of TIG welding are listed as

- Lower speed of metal stacking comparing with other methods,
- Expensive application for part with thicker cross section,
- Need for shield metal gas,
- Hard to use in outdoors,
- Not used for tin and lead.

2.3. Joint Preparation

Joint preparation is fundamental in welding. Welding method and metal thickness should be considered while welding joint preparation design. Accessibility to welding area for welder and to provide adequate fusion during holding electrode are also important parameters of welding joint design. Joint preparation could be expensive process. Base metal involvement to work piece may be preferable to use less filler metal. During welding joint design, cleanliness of both base metal and filler metal is crucial. Any external contamination could affect welding quality and create weld defects. Base metal and filler metal should be purified before welding joint preparation from oil, grease, dirt, rust and corrosion (Weman, 2012; Singh, 2016). Figure 2.5 shows some joint types example.

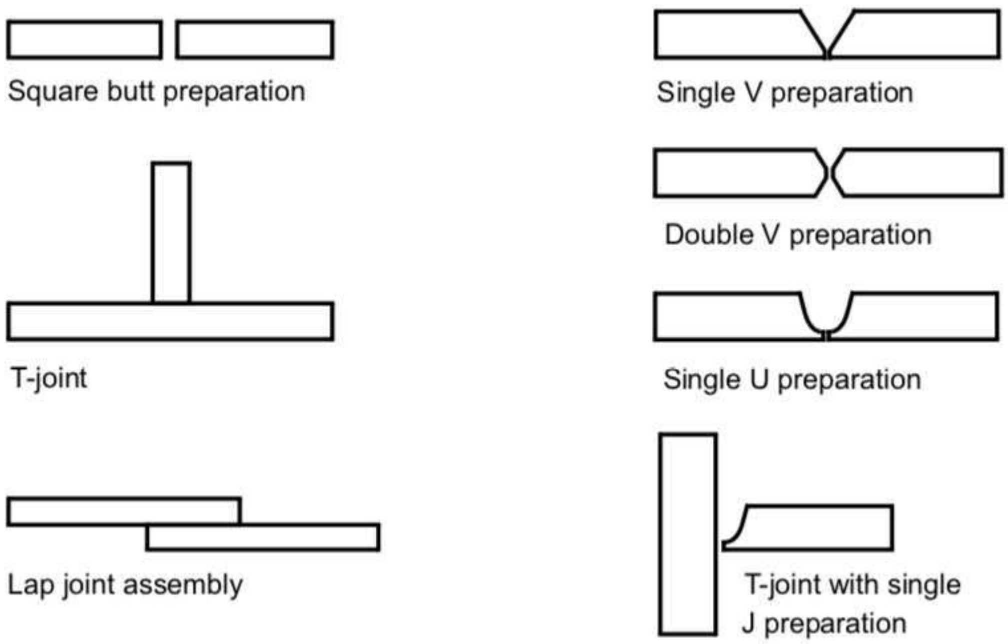

Figure 2.5. Examples of joint types

(Source: Weman, 2012)

.

CHAPTER 3

REGRESSION

3.1. Introduction

According to American Heritage Dictionary, regression is that a technique for predicting the value of a dependent variable as a function of one or more independent variables in the presence of random error. It is one of the most preferred tool in order to easily transfer a physical event to a mathematical model. Output can be provided with a single input or model can be created with more than one input. The relationship between these numerical inputs and output is achieved by single or multiple regression analysis. (Mishra, 2018).

Coefficient of determination, which is known as r-square R^2, is widely used statistic in regression analysis. R^2 is defined as variation ratio of the output data Y which is generated by the regression model. Calculation of R^2 is done by using the following formula:

$$R^2 = SSM/SST = 1 - SSE/SST \quad (3.1)$$

where

Sum of Squares Total: $SST = \Sigma (Y - \bar{Y})^2$, where $\bar{Y}$ is the overall average.

Sum of Squares Model: $SSM = \Sigma (\hat{Y} - \bar{Y})^2$, where $\hat{Y}$ is predicted value.

Sum of Squares Error: $SSE = \Sigma (Y - \hat{Y})^2$

The adjusted R-squared is a modified version of R-squared that has been adjusted for the number of predictors in the model. When the new term of the equation enhances the model more than expected by incidentally, the adjusted R-squared increases. If the new term makes model worse than expected, the adjusted R-squared decreases. The adjusted R-squared formula is given as

$$R^2_{adj} = 1 - [(1 - R^2)(N - 1) / (N - k - 1)] \quad (3.2)$$

where N is total sample size, k is number of predictors.

The least square is a mathematical procedure for finding the best-fitting curve to a given set of points by minimizing the sum of the squares of the offsets of the points from the curve. Best fitting is a possible value, which represented fitted function. The sum of the squares of the offsets is used instead of the offset absolute values because this allows the residuals to be treated as a continuous differentiable quantity. However, because squares of the offsets are used, outlying points can have a disproportionate effect on the fit, a property which may or may not be desirable depending on the problem at hand.

The linear least squares fitting technique is the simplest and most commonly applied form of linear regression and provides a solution to the problem of finding the best fitting straight line through a set of points. Standard forms for exponential, logarithmic, and power laws are often explicitly computed. The formulas for linear least squares fitting were independently derived by Gauss and Legendre.

For nonlinear least squares, fitting to a number of unknown parameters, linear least squares fitting may be applied iteratively to a linearized form of the function until convergence is achieved. However, it is often also possible to linearize a nonlinear function at the outset and still use linear methods for determining fit parameters without resorting to iterative procedures. This approach does commonly violate the implicit assumption that the distribution of errors is normal, but often still gives acceptable results using normal equations, a pseudoinverse, etc. Depending on the type of fit and initial parameters chosen, the nonlinear fit may have good or poor convergence properties. If uncertainties (in the most general case, error ellipses) are given for the points, points can be weighted differently in order to give the high-quality points more weight. (Weisstein, 2019)

3.2. Simple Linear Regression

Simple linear regression is used for the function what obtained using a single input variable, x. Simple linear regression defines an equation that has response variable, Y as output and input variable as given below

$$Y = \beta_0 + \beta_1 x \tag{3.3}$$

where β_0 is the constant term and β_1 gives the slope of the graph shown in Figure 3.1. Coefficients are estimated by regression analysis minimizing the *Sum of Square Error, SSE* as follow:

$$SSE = \Sigma (Y - (\beta_0 + \beta_1 x))^2 \tag{3.4}$$

Here $\beta_0 + \beta_1 x$ is the estimated Y which is denoted by $\hat{Y}$. Aim of the regression is to approximate actual data Y and predicted data $\hat{Y}$.

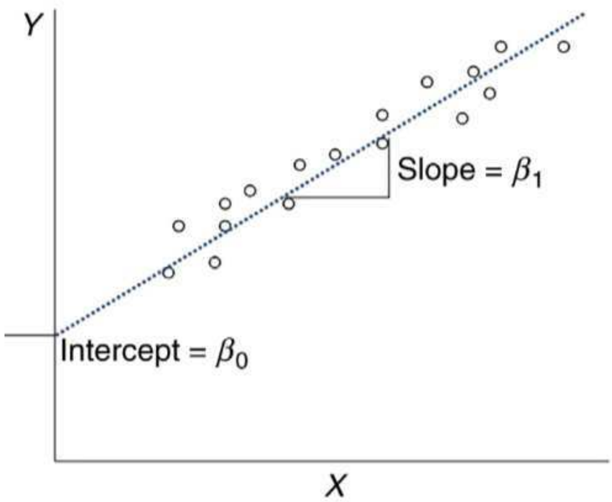

Figure 3.1 Slope and Constant term for Line graph

(Source: Pinder, 2017)

3.3. Multiple Linear Regression

More than one input affect result in process that should be taken under control. As a mathematical explanation, Variation in the Y data is explained with more than one x variables. Multiple regression is defined as regression has several x variables. General multiple linear regression equation below as:

$$\mathrm{Y} = a_0 + a_1 x_1 + a_2 x_2 \dots + a_n x_n \tag{3.5}$$

3.4. Simple Nonlinear Regression

Nonlinear regression model cannot be defined by nonlinear equation that cannot be linearized and does not obey the superposition and scaling rules. (Kissell, 2017; Aster, 2019). Simple nonlinear regression for a function that has only one input variable can be expressed as:

$$\mathrm{Y} = a_0 + a_1 x^2 \tag{3.6}$$

3.5. Multiple Nonlinear Regression

Multiple linear regression models are nonlinear equations that have more than one input. Equation 3.5 shows polynomial nonlinear regression model expression.

$$\mathrm{Y} = a_0 + a_1 x_1 + a_2 x_2^2 \dots + a_n x_n^n \tag{3.7}$$

Multiple nonlinear regression models could be trigonometric functions, logarithms, exponentials, rational polynomial etc. Some examples of multiple nonlinear regression models are as:

$$\mathrm{Y} = a_0 + a_1 \sin x_1 + a_2 \sin x_2 + a_3 \cos x_1 + a_4 \cos x_2 \tag{3.8}$$

$$\mathrm{Y} = a_0 + a_1 \ln x_1 + a_2 \ln x_2 \tag{3.9}$$

where a_i terms are constant and x_i terms are input variables.

3.6 Mathematica Implementation

A nonlinear least-squares model is an extension of the linear model where the model need to be linear combination of basis function. The errors are still assumed to be independent and normally distributed. Models of this type can be fitted using the *NonlinearModelFit* function in Wolfram Mathematica. Nonlinear models have the form $y = f(x_1 \ldots x_i, B_1 \ldots B_i)$ where y is the fitted or predicted value, the B are parameters to be fitted, and the x are predictor variables. As with any nonlinear optimization problem, a good choice of starting values for the parameters may be necessary. Starting values can be given using the same parameter specifications as for *FindFit*. Options for model fitting and for model analysis are shown in Table 3.1.

Table 3.1 Options for model fitting

Option Name	**Default Value**	**Option Explanation**
AccuracyGoal	Automatic	The accuracy sought
ConfidenceLevel	95/100	Confidence level to use for parameters and predictions
EvalutionMonitor	None	Expression to evaluate whenever expr is evaluated
MaxIterations	Automatic	Maximum number of iterations to use
Method	Automatic	Method to use
PrecisionGoal	Automatic	The precision sought
StepMonitor	None	The expression to evaluate whenever a step is taken
VarianceEstimatorFunction	Automatic	Function for estimating the error variance
Weights	Automatic	Weights for data elements
WorkingPrecision	Automatic	Precision used in internal computations

General numeric options such as *AccuracyGoal, Method*, and *WorkingPrecision* are the same as for *FindFit*. The *Weight* option specifies weight values for weighted nonlinear regression. The optimal fit is for a weighted sum of squared errors. All other options can be relevant to computation of results after the initial fitting. They can be set within *NonlinearModelFit* for use in the fitting and to specify the default settings for results obtained from the *FittedModel* object. These options can also be set within an already constructed *FittedModel* object to override the option values originally given to *NonlinearModelFit*.

CHAPTER 4

OPTIMIZATION

4.1. Introduction

The main issue is to generate most profit with least cost and time in every area of industry. Optimization is to find minimum or maximum value of function that is modeled mathematically which has well defined inputs and output in affecting boundary constrains. The prime target of engineering is to optimize parameters like weight, strength, time, etc. by using optimization methods. It is impossible to solve the entire optimization problem that engineering has with a single solution method. Several optimization methods are developed to examine different kinds of optimization problems for mathematically modeled function (Rao, 2009).

Studies of Newton, Lagrange, and Cauchy were found of the optimization during historical development. Important steps were taken about unconstrained optimization after studies of Newton, Lagrange, and Cauchy in United Kingdom in the 1960s. Nontraditional optimization methods became popular to solve complex engineering problems in modern times. Stochastic algorithm is a nontraditional and non-deterministic algorithm, which relies on probabilistic operations. Stochastic methods, which are constantly preferred, are as

Differential Evolution Algorithm (DE),
Partial Swarm (PS),
Simulated Annealing Algorithm (SA)
Random Search Algorithm (RS)
Genetic Algorithm (GA)

In this study, regression models of the weld bead geometric parameters are designed and optimization of these parameters are achieved by using DE, NM, SA, and RS stochastic methods. Stochastic methods are preferred because it is not possible to solve optimization problem that included discrete-continuous mixed domain and/or integer, nonlinear constraint, nonlinear objective function with conventional optimization methods.

4.2. Defining an Optimization Problem

The design factor (x), objective function f(x), and constraints as $g_j(x)$ and $l_j(x)$ are determined elements of optimization problems. Not every optimization problem should have constraints. A basic constrained optimization problem is stated below.

Minimize: $f(x_1, x_2, \ldots, x_n)$

Constraint: $h_j(x) = 0, \quad j = 1, 2, \ldots$
$g_j(x) < 0, \quad j = 1, 2, \ldots$

Design vector x is an input of process that willing to model. The design vector is defined by design variables. Commonly, there are more than one design variables in an engineering system. Every design variables comes with physical constraints in a real life process. Characterization and limitation of the system are represented by constraints.

4.3. Stochastic Search Algorithms

In this thesis, following algorithms are used for minimization of one of the weld bead geometric dimensions, which is front width. Information about algorithm parameters for each method in Wolfram Mathematica software is shown in Table 4.1. In the following subsections, brief information about these algorithms are given.

Table 4.1 Options for NM, DE, SA, and RS in Wolfram Mathematica

Option Name	NM	DE	SA	RS	Option Explanation
"ContractRatio"	0.5		-	-	ratio used for contraction
"ExpandRatio"	2.0		-	-	ratio used for expansion
"InitialPoints"	Auto	Auto	Auto	Auto	set of initial points
"PenaltyFunction"	Auto	Auto	Auto	Auto	function applied to constraints to penalize invalid points
"PostProcess"	Auto	Auto	Auto	Auto	whether to post-process using local search methods
"RandomSeed"	0	0	0	0	starting value for the random number generator
"ReflectRatio"	1.0		-	-	ratio used for reflection
"ShrinkRatio"	0.5		-	-	ratio used for shrinking
"Tolerance"	0.001	0.001	0.001	0.001	tolerance for accepting constraint violations
"CrossProbability"	-	0.5	-	-	probability that a gene is taken from xi
"ScalingFactor"	-	0.6	-	-	scale applied to the difference vector in creating a mate
"SearchPoints"	-	Auto	Auto	Auto	size of the population used for evolution
"LevelIterations"	-	-	50	-	maximum number of iterations to stay at a given point
"PerturbationScale"	-	-	1.0	-	scale for the random jump

4.3.1. Differential Evolution Algorithm (DE)

Differential Evolution algorithm, which is vectorial metaheuristic algorithm that has several variables, is used in different kinds of area because of its converging characteristic. It is advanced in 1996 and 1997 studies that are owned by R. Storn and K. Price. DE is an algorithm that uses real numbers and has resemblances with pattern search and genetic algorithm in areas as crossbreeding and mutation. DE takes action in every dimension of solution. It uses difference vector of randomized two populations in order to have different another vector (Yang, 2014). Flowchart of Differential Evolution is shown in Figure 4.1.

In Mathematica implementation of MDE algorithm, it considers a population of r points, $\{ x_1, x_2, \ldots, x_j, \ldots, x_r\}$. It is crucial that r should be much higher than the number of design variables. At the iteration proses, firstly, the algorithm generates a new population that is produced by selecting random points. By introducing the real scaling factor as "*rsf*" and defining $x_{rsf} = x_w + rsf\,(x_u - x_v)$, i^{th} iteration points can be obtained from the previous population. Secondly, a new point x_{new} is established by selecting j^{th} coordinate from θ_{rsf} with probability P. In Mathematica software, P can be adjusted by the option "CrossProbability". In that step, if the constraint $f(x_{new})<f(x_i)$ is valid then x_i is taken instead of x_{new} in the population. Stopping criteria for this process is that if the difference between the optimum output values at the new and old populations, the difference between two (the new and old) points the new best points are less than the tolerances provided by the parameters which specifies how many effective digits of accuracy and precision should be sought in the final result.

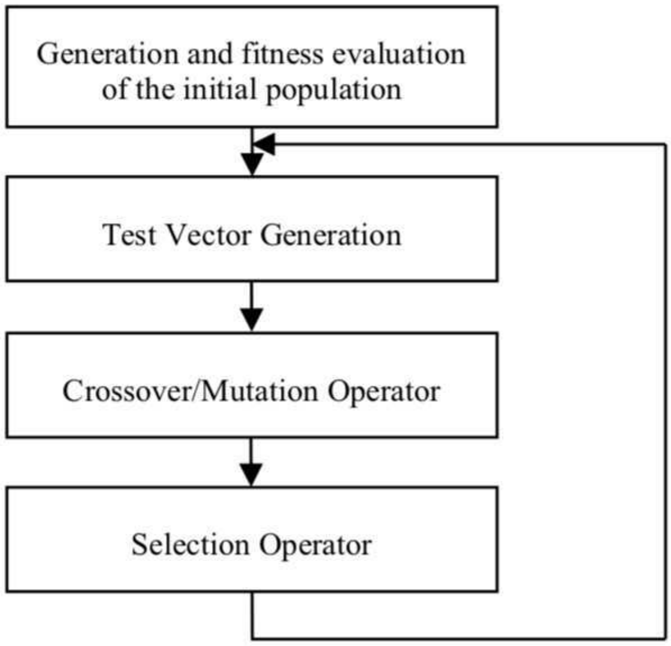

Figure 4.1 Differential Evolution Algorithm Flowchart

(Source: Cortes-Antonio, 2014)

4.3.2. Nelder Mead Algorithm (NM)

Nelder Mead algorithm, which is known as simplex method, arranges itself local for reaching final minimum. Due to local minimum adaptation, Nelder Mead algorithm is not a useful method for optimization problems have several local points. It is developed by J. A. Nelder and R. Mead in 1965 with a guidance study of Spendly et al. (1962). It is used to minimize simplex with n variables. In standard Nelder Mead, it was not created for problems that have constraint. Nelder Mead is an iterative algorithm and has four control parameters. Control parameters of Nelder Mead algorithm are reflection factor, expansion factor, construction factor, and shrinkage factor (Xu et al., 2019). Steps of Nelder Mead algorithm is in below.

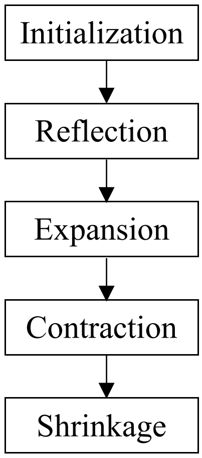

Figure 4.2 Nelder Mead Algorithm Flowchart

(Source: Wang et al., 2011)

One of the simple direct search method is Nelder Mead optimization algorithm. Therefore, it does not require any derivative information and starts with a simplex for minimization of the function. The iteration maintain up to the simplex becomes flat. It means that the resulting value of the function is almost the same at all the vertices. The iteration steps of Nelder Mead algorithm are Ordering: Centroid, Transformation. In the present version of the algorithm, a penalty function is added to the flow in order to solve prescribed constrained minimization problem. Construction of the initial working simplex S is a first step. Second, minimizing the function moves the search course away from the peak, which is the worst function value. This is achieved by yielding a reflected and improved point. In the present paper, a modified version of the NM algorithm which can solve the optimization problems containing non-linear constraints, mixed integer and continuous design variables has been used.

4.3.3. Simulated Annealing Algorithm (SA)

Simulated Annealing is an algorithm that developed for optimization problems have global optima which is inspired by annealing process of metals that explains slow cooling down. This algorithm is an ideal method to analyze complex and difficult problems that cannot be solved with other methods. Metal should be permitted to cool down by itself to reduce the system its minimum energy. This method is used to find global optima of nonlinear functions. Mathematica implementation of Modified Simulated Annealing (MSA) can be briefly explained as follows:

Firstly, an initial guess is introduced as x_{in}. Secondly, a new point, x_{new}, is produced in the neighborhood of the current point, x at each iteration so far, x_{best}, is also tracked. The main idea is here that the radius of the neighborhood reduces with the iteration. If $f(x_{new}) <= f(x_{best})$, x_{new} replaces x_{best} and x. Otherwise, x_{new} replaces x with a probability. The distance between the current and new points can be calculated by Boltzmann's probability distribution function$e^{B(i,\Delta f,f_0)}$.

In this distribution "*B*" is the function characterized by Boltzmann Exponent, "*i*" is the current iteration, "*Δf*" is the change in the fitness function value, and "f_0" represents the value of the objective function from the $(i\text{-}1)^{th}$ iteration. B is $\frac{-\Delta f \log(i+1)}{10}$ if it is not introduced by the user. Instead of only one initial guess the Mathematica command "Simulated Annealing" uses two or more starting points. The option Search Points give the number of initial points, and it is calculated as *min (2r, 50)*. In this expression, the number of variables is denoted by the term *r*. According to the variation of the initial points, the process sustains successively up to the iteration number limits. "*Level Iterations*" option gives the number of iterations to converges to a point, or the technique stays at the same point given before.

The flowchart of a Simulated Annealing algorithm is presented in Figure 4.3, so as to follow the procedure of the algorithm readily.

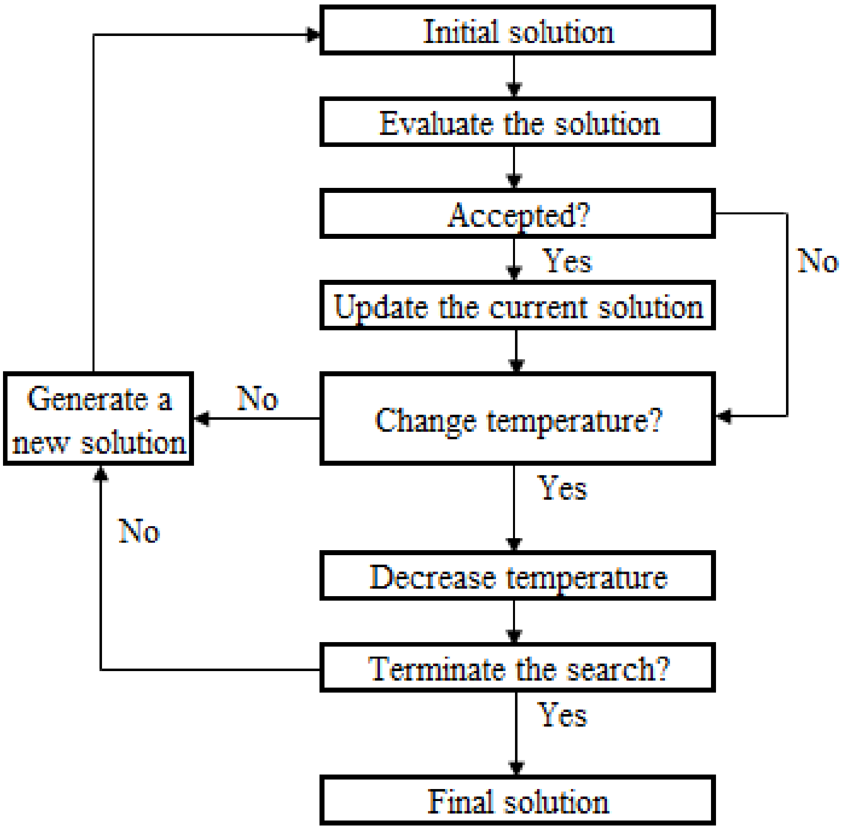

Figure 4.3 Simulated Annealing Algorithm Flowchart
(Source: Pham and Karaboga, 2012)

4.3.4. Random Search Algorithm (RS)

RS method (also known as a Monte-Carlo method) is a stochastic algorithm and different from the most deterministic maximum search methods, such as Branch and Bound, Interval Analysis, and Tunneling methods. The solution procedure of the algorithm provides some ad- vantages; for example: since small step methods can, find only the top of a local peak, it should be combined with some sort of true search procedure when a search for the absolute maximum of a multimodal function is required. In the random process, there are a number of standard techniques and programs based on a pseudo-random number generator. The resulting values have to be scaled and transformed in order to produce an approximation to any desired distribution. The main advantage which provides to appropriate usage of RS algorithms is that it is possible to reach the global optimum for non-convex, non- differentiable objective functions including continuous, discrete do- mains, or mix of them for large-scale problems. Another advantage of RS method is that they are relatively easy to implement on complex problems. Generally, it is known that RS algorithms perform well and are “robust” in the sense that they give useful information quickly for ill-structured global optimization problems. The algorithm used in the present study follows the procedure given in Figure 4.4. Detail discussion of random search method can also be found in Karnopp (1963), Zabinsky (2009).

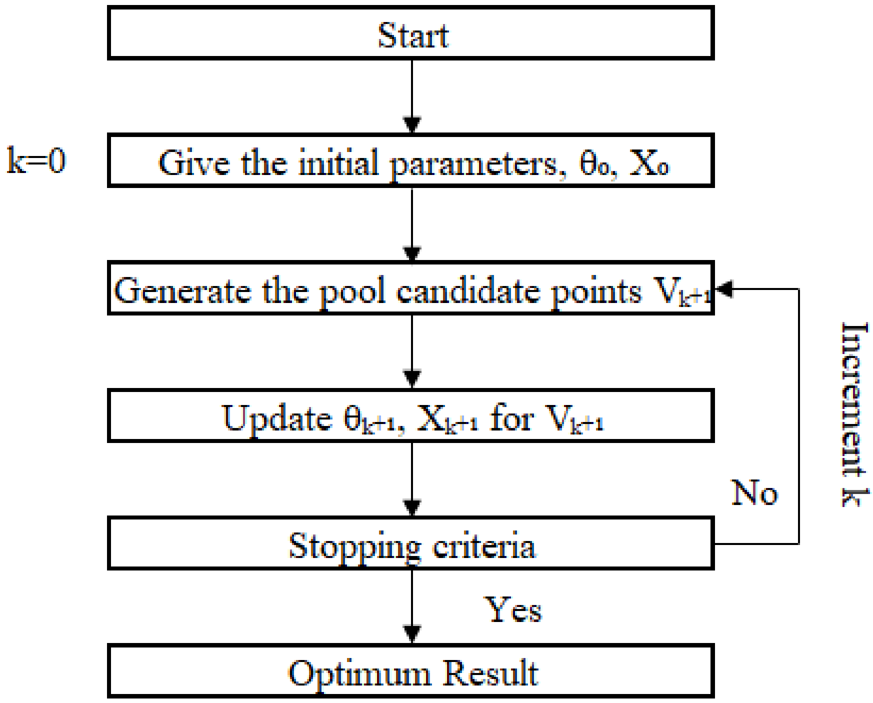

Figure 4.4 Random Search Algorithm Flowchart

(Source: Zabinsky, 2009)

CHAPTER 5

RESULT AND DISCUSSION

5.1. Problem Statement and Modelling

Welding process, comprised by various fields like aircraft engines, internal and external parts of vehicles, bridges, towers, heat exchangers, and valves is a complex application. Expectation for qualified welding is met with physical and micro-structural requirements in minimum material condition by decreasing cost.

Juang et al. (1998) studied with five input variables of TIG welding which are welding speed, wire feed rate, cleaning percentage, gap, and welding current. Dutta and Pratihar studied with Juang's experiment data. However, full factorial DOE is applied to select 36 data from 72 data. In this thesis, set of data of Dutta and Pratihar's is used. In their study, they selected wire feed rate as 2. In this thesis, TIG welding process has been modeled by using regression analysis. Then, the response equation (model equation for front width) as a function of input variables were minimized by using optimization algorithms. Welding speed, wire feed rate, % cleaning, gap and welding current are taken as input variables. Response variables are front height, front width, back height, and back width. Figure 5.1 shows a schematic diagram for the weld bead geometric parameters in TIG welding process.

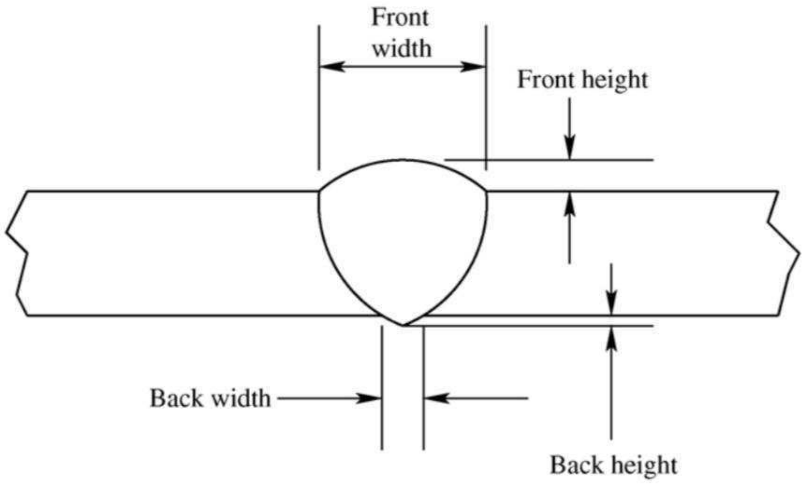

Figure 5.1 Geometric dimensions of weld bead
(Source: Dutta and Prahitar, 2006)

Input and output variables of TIG welding process is presented in Figure 5.2. The ranges of the input parameters based upon experimental data taken from Dutta and Pratihar (2006) studies for the analysis are given in Table 5.1.

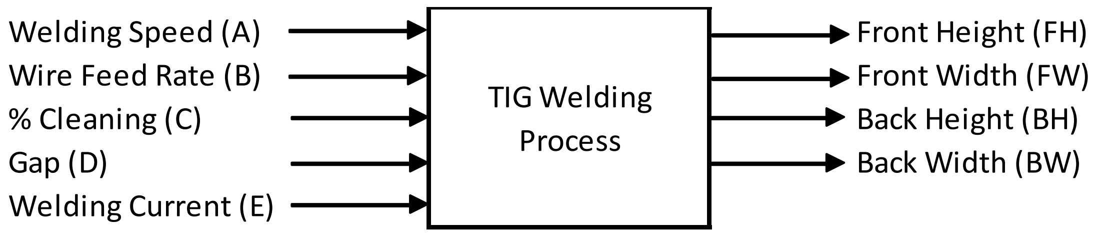

Figure 5.2 TIG Welding Process Variables
(Source: Dutta and Prahitar, 2006)

Experimental data set is shown in Table 5.2. Within this context, four response variables of weld bead geometry that are front height, front width, back height, and back width are designed by regression analysis with using elementary function models. First order versions of these functions are shown in Table 5.3. In this thesis, elementary functions are used to model physical events which are front height, front width, back height and back width with multiple input variables. Rational version of elementary functions is also implemented. The reason of rational model trail is boundedness control of rational models. It prevented that result could go to infinity. The limit of rational model usage is the values that makes denominator zero.

Table 5.1 Input parameters

(Source: Dutta and Pratihar, 2006)

Input Parameters	Units	Notation	Minimum Value	Maximum Value
Welding Speed	cm/min	A	24	46
Wire Feed Rate	cm/min	B	1.5	2.5
% Cleaning		C	30	70
Gap	mm	D	2.4	3.2
Welding Current	A	E	80	110

Table 5.3 Forms of different models considered

Model Name		Formula
First Order Logarithmic	Y=	$a_0 + a_1 \ln x_1 + a_2 \ln x_2 + a_3 \ln x_3 + a_4 \ln x_4 + a_5 \ln x_5$
First Order Logarithmic Rational	Y=	$\frac{a_0 + a_1 \ln x_1 + a_2 \ln x_2 + a_3 \ln x_3 + a_4 \ln x_4 + a_5 \ln x_5}{b_0 + b_1 \ln x_1 + b_2 \ln x_2 + b_3 \ln x_3 + b_4 \ln x_4 + b_5 \ln x_5}$
First Order Polynomial	Y=	$a_0 + a_1 x_1 + a_2 x_2 + a_3 x_3 + a_4 x_4 + a_5 x_5$
First Order Polynomial Rational	Y=	$\frac{a_0 + a_1 x_1 + a_2 x_2 + a_3 x_3 + a_4 x_4 + a_5 x_5}{b_0 + b_1 x_1 + b_2 x_2 + b_3 x_3 + b_4 x_4 + b_5 x_5}$
First Order Trigonometric	Y=	$a_0 + a_1 \mathrm{Sin}(x_1) + a_2 \mathrm{Sin}(x_2) + a_3 \mathrm{Sin}(x_3) + a_4 \mathrm{Sin}(x_4) + a_5 \mathrm{Sin}(x_5) + a_6 \mathrm{Cos}(x_1) + a_7 \mathrm{Cos}(x_2) + a_8 \mathrm{Cos}(x_3) + a_9 \mathrm{Cos}(x_4) + a_{10} \mathrm{Cos}(x_5)$
First Order Trigonometric Rational	Y=	$\frac{a_0 + a_1 \mathrm{Sin}(x_1) + a_2 \mathrm{Sin}(x_2) + a_3 \mathrm{Sin}(x_3) + a_4 \mathrm{Sin}(x_4) + a_5 \mathrm{Sin}(x_5) + a_6 \mathrm{Cos}(x_1) + a_7 \mathrm{Cos}(x_2) + a_8 \mathrm{Cos}(x_3) + a_9 \mathrm{Cos}(x_4) + a_{10} \mathrm{Cos}(x_5)}{a_0 + a_1 \mathrm{Sin}(x_1) + a_2 \mathrm{Sin}(x_2) + a_3 \mathrm{Sin}(x_3) + a_4 \mathrm{Sin}(x_4) + a_5 \mathrm{Sin}(x_5) + a_6 \mathrm{Cos}(x_1) + a_7 \mathrm{Cos}(x_2) + a_8 \mathrm{Cos}(x_3) + a_9 \mathrm{Cos}(x_4) + a_{10} \mathrm{Cos}(x_5)}$

Table 5.2 Experimental data used to carry out regression analysis
(Source: Dutta and Pratihar, 2006)

Inputs					Outputs			
A	B	C	D	E	FH	FW	BH	BW
24	2	30	2.4	80	-0.066	6.123	0.801	5.541
24	2	30	3.2	80	0.114	5.979	0.682	4.633
24	2	70	2.4	80	-0.213	7.424	0.806	7.026
24	2	70	3.2	80	0.034	7.516	0.557	7.480
24	2	30	2.4	95	-0.167	8.481	0.713	8.340
24	2	30	3.2	95	-0.296	8.928	0.807	8.640
24	2	70	2.4	95	-0.219	9.677	0.688	9.717
24	2	70	3.2	95	-0.448	10.523	1.005	11.088
24	2	30	2.4	110	-0.281	10.871	0.713	11.142
24	2	30	3.2	110	-0.452	10.830	0.803	11.370
24	2	70	2.4	110	-0.651	13.986	1.090	14.146
24	2	70	3.2	110	-0.74	12.273	1.148	12.712
35	2	30	2.4	80	0.144	5.474	0.425	5.057
35	2	30	3.2	80	0.224	5.449	0.379	3.884
35	2	70	2.4	80	0.023	5.758	0.515	4.970
35	2	70	3.2	80	0.041	5.758	0.540	4.768
35	2	30	2.4	95	-0.094	6.665	0.613	6.304
35	2	30	3.2	95	-0.154	7.402	0.564	7.440
35	2	70	2.4	95	-0.179	7.614	0.610	7.557
35	2	70	3.2	95	-0.005	7.506	0.457	7.310
35	2	30	2.4	110	-0.433	8.011	0.868	8.047
35	2	30	3.2	110	-0.449	8.473	0.780	8.466
35	2	70	2.4	110	-0.396	9.652	0.782	10.277
35	2	70	3.2	110	-0.553	9.773	0.847	10.427
46	2	30	2.4	80	0.454	5.581	0.315	3.046
46	2	30	3.2	80	0.193	4.645	0.332	2.810
46	2	70	2.4	80	0.023	5.646	0.584	4.034
46	2	70	3.2	80	0.219	5.538	0.363	2.857
46	2	30	2.4	95	0.057	5.600	0.495	4.836
46	2	30	3.2	95	0.155	6.002	0.351	4.922
46	2	70	2.4	95	-0.189	5.859	0.729	5.201
46	2	70	3.2	95	-0.182	6.124	0.569	5.299
46	2	30	2.4	110	-0.386	6.927	0.748	6.775
46	2	30	3.2	110	-0.154	6.877	0.539	6.335
46	2	70	2.4	110	-0.350	7.630	0.650	7.869
46	2	70	3.2	110	-0.225	7.553	0.557	7.707

5.2. Selecting Model and Effects of Independent Input Variables

Example of Wolfram Mathematica code to find conventional R^2, R^2 adjusted, R^2 training, and R^2 testing, which is constructed with inputs given in Table 5.1 and mathematical models in Table 5.2, is shown in Appendix A.

Coefficient of determination R^2 and R^2 adjusted values are listed in Appendix B. These values are generated using traditional regression analysis and models depicted in Table 5.2. Models that are generated with standard regression approach are not effective to state physical problem enough by comparing R^2 and R^2 adjusted values. It is seen that sixth order logarithmic and polynomial models could represent exactly physical phenomena for front height. Although fourth order trigonometric model could represent the same physical phenomena for front height, logarithmic and polynomial models requires increase in order. Fourth order rational trigonometric, sixth order logarithmic and polynomial, and fourth order trigonometric models are represented front width with a giving R^2 equals to 1 that means theoretically predicted response values and actual response values gave the same result. Trigonometric models gave the value of 1 for coefficient of determination in fourth, fifth, and sixth order. Fifth and sixth order rational trigonometric models gives result just around 0.23. It because model showed oscillation behavior more than that the event needs. Sixth order polynomial, rational polynomial, logarithmic, and rational logarithmic models represented physical event for both back height and back width with one hundred percent agreement. Trigonometric and rational trigonometric models gave the value of 1 for coefficient of determination with fourth order. However, fifth and sixth order trigonometric rational models did not match with the physical events sufficiently.

Neuro-regression, which is hybrid application of regression analysis and artificial neural network, is performed. Four output variables are modeled by using neuro-regression analysis. Four input variables are taken minimum to see effect of the other one among the five inputs. Subsequently, experimental data set divided randomly into two sets of data, 80 percent and 20 percent of data. Regression analysis without using 20 percent of data is studied, and it coefficients of determination are found. 20 percent of data is substituted to models and new testing coefficients of determination are found. Comparison between training and testing coefficients R^2 shows reliability of the models.

Appendix C indicates values of R^2 training and R^2 testing thereafter hybrid study. R^2 training should be near to one and R^2 training and R^2 testing should be converge each other while selecting optimal model. Models are selected for all four output variables by examining and comparing result of R^2 training and R^2 testing, as given in Appendix C. First order multiple linear model for front height, third order multiple polynomial model for front width, first order multiple trigonometric nonlinear model for back height, and first order multiple linear model for back width are chosen. Logarithmic models made R^2 training results increase with increasing order from first to sixth. R^2 testing results are decreased by order for front height. R^2 training value is rising with order from first to sixth in rational logarithmic model; nevertheless, R^2 testing did not converge with R^2 training. R^2 training and R^2 testing results converged to both the value of 1 and each other for the first order polynomial model. The remaining orders for polynomial models did not represent phenomena as the first order model did. R^2 training results for third or higher order trigonometric and rational trigonometric models gave value of 1. However, none of the R^2 testing values could demonstrate the event in the way of the first order linear model did. First to sixth order logarithmic and rational logarithmic models showed above 99 % match for R^2 training in front width, although R^2 testing could not perform over 85 %. Third order polynomial model represented the phenomena well by converging to value of 1 and each other around 0.89. All six model types and six orders for back height demonstrated 97 % and above similarity for predicted and actual outputs. Values of R^2 testing gave results around 0.77 for first order logarithmic model; but with increasing order, R^2 training decreased. Negative value of results could be seen for R^2 testing values for all model in back height, because of values deviation and nature of process. R^2 training indicated increasing behavior for logarithmic, polynomial and trigonometric models of back width. R^2 testing values of back width decreased with increasing order by the opposite way of R^2 training. Independent results for R^2 testing could be investigate from order in all rational models. R^2 testing took negative values after second order for model that is rational trigonometric.

Effects of input variables, which are welding speed, wire feed rate, % cleaning, gap, and welding current on four response variables, which are front height, front width, back height, and back width are investigated separately and presented in Figures 5.3- 5.6. In all these figures, while investigating the effect of each parameter on response function, the other parameters are kept constant as welding speed of 24 cm/min, wire feed rate of 2 cm/min, % cleaning of 30, gap of 2.4 mm, and welding current of 80.

5.2.1. Effects of Independent Input Variables on Front Height

It can be seen from the Figure 5.3 (a) that front height is increased by changing welding speed minimum to maximum while the other parameters are kept constant with wire feed rate of 2 cm/min, % cleaning of 30, gap of 2.4 mm, and welding current of 80 A. Wire feed rate raise changed front height between -0.1 and 0.2 and by this change, it could be seen under zero values for front height as a relationship between wire feed rate and front height that is shown in Figure 5.3. Low values of front height is achieved by getting higher value of percentage cleaning on the contrary of weld speed and wire feed rate. The deviation is occurred between -0.06 and 0.06. Front height increased with higher the gap between components that desired to weld, as shown in Figure 5.3. Increasing welding current made front height minimum similarly with percentage cleaning as demonstrated in Figure 5.3. Welding current affected front height aggressively unlike the effects of other four inputs. It developed 0.5 error by giving study range between -0.4 and 0.1.

5.2.2. Effects of Independent Input Variables on Front Width

Front width could not show linear response in study with weld speed between 24 and 46 cm/min. Front width, which decreased in a certain range with increasing weld speed and then took minimum value with maximum weld speed is indicated in Figure 5.4. Wire feed rate gave minimum front width with minimum value of itself by drawing concave curve. It studied in range of 0.8 by moving from 4.8 to 5.6 approximately as shown in Figure 5.4. This shows increasing in front width with increasing percentage cleaning. Increasing gap between work pieces increased front width as demonstrated in Figure 5.4. Welding current effect gave more aggressive result for front width similar with front height. However, welding current, which decreased front height at maximum value of itself, made front width minimum with minimum state of it.

5.2.3. Effects of Independent Input Variables on Back Height

Deviation of weld speed creates sinus curve with corners on back height. As it is seen from Figure 5.5., back height took minimum values around 28, 46, and between 35 and 39 cm/min. Increasing wire feed rate made back height higher. Figure 5.5 showed that wire feed rate changed back height in 0.2 range. Percentage Cleaning, which moved between % 30 and 70, affected back height with sinus curve with corners in the same way with weld speed as indicated in Figure 5.5. Raising gap between materials reduced back height with nonlinear curve. This decrease occurred proportionally in range of 0.15 (Figure 5.5). Low welding current looks like that it reduced back height. It is seen that back height decreased around 100 A with large sinus curve in Figure 5.5.

5.2.4. Effects of Independent Input Variables on Back Width

Increasing welding speed decreased back width in an opposite way of front height. The welding speed affected back width aggressively with a variation as demonstrated in Figure 5.6. Wire feed rate also decreased back width with an increasing change. However, the decrease in back width showed low deviation and the wire feed rate was not effective as weld speed (Figure 5.6). Percentage cleaning affected back width with linear increase from 6 cm to 8 cm approximately as shown in Figure 5.6. Gap created linear effect as the same way percentage cleaning did. Welding current increased back width from 6 cm to 12 cm by increasing welding current itself from 80 A to 110 A. It can be seen that welding current is more effective than other input variables by comparing graph values of back width with 6 cm deviation approximately.

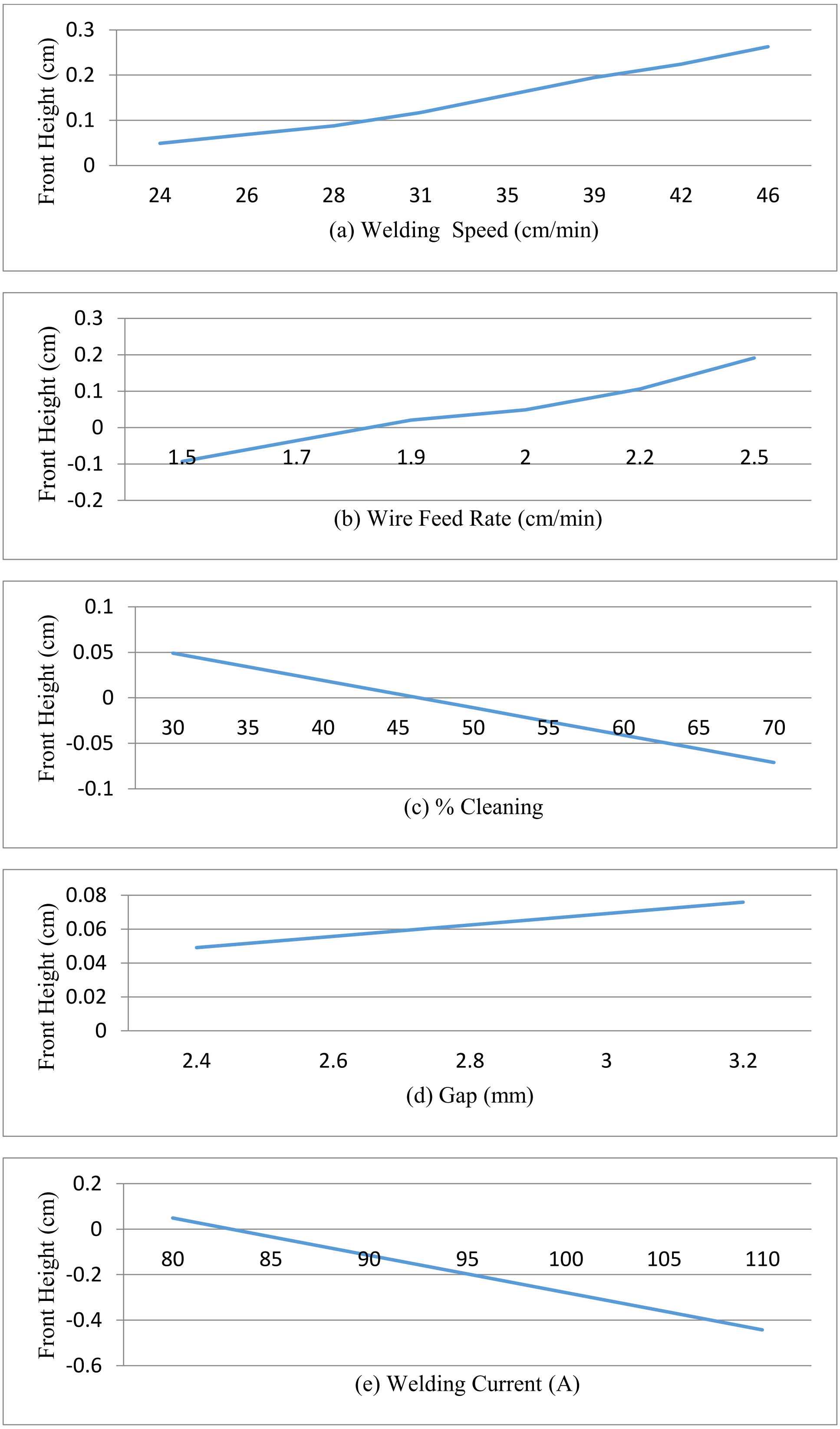

Figure 5.3 Effects of independent input variables on Front Height

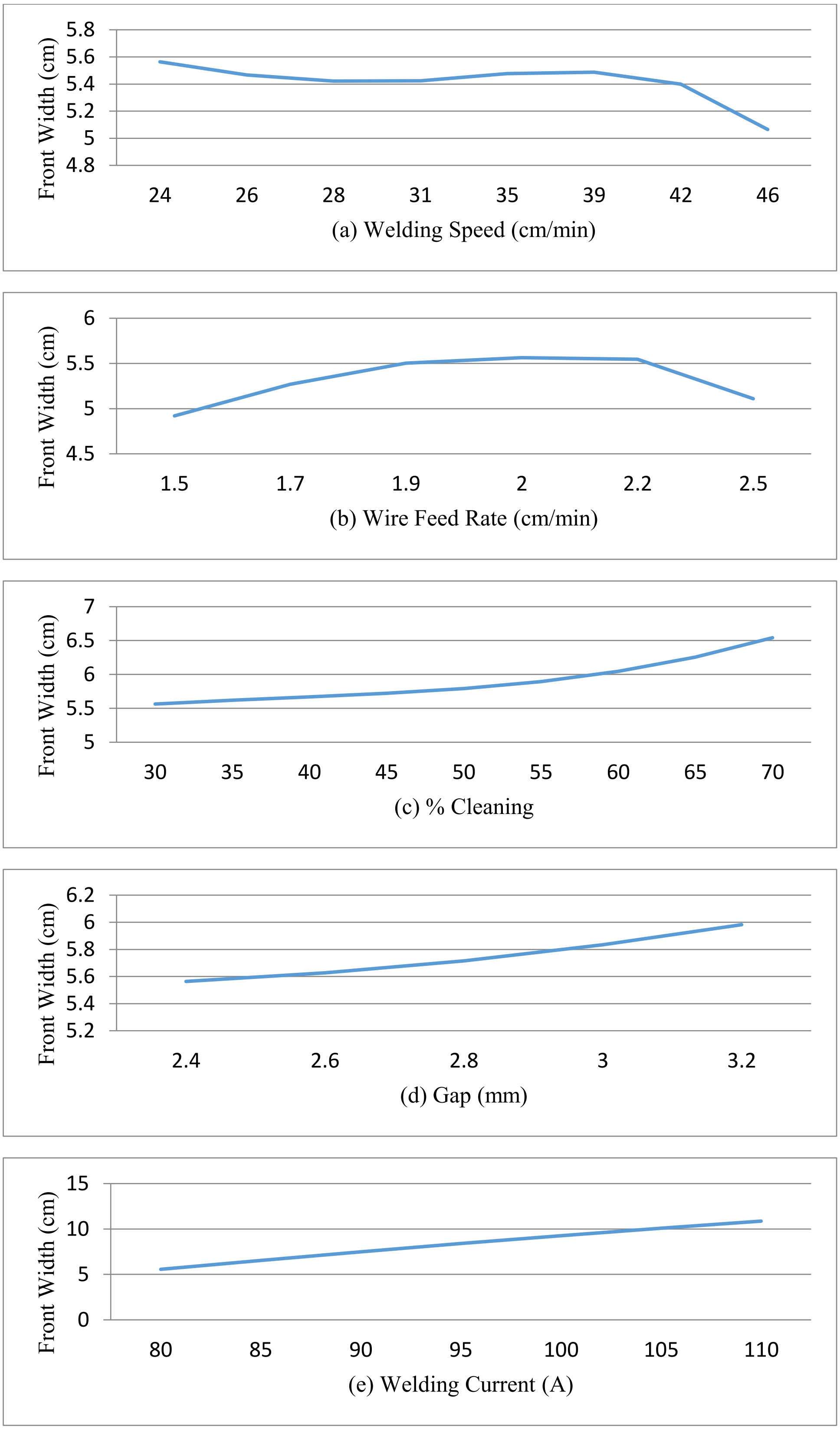

Figure 5.4 Effects of Independent Input Variables on Front Width

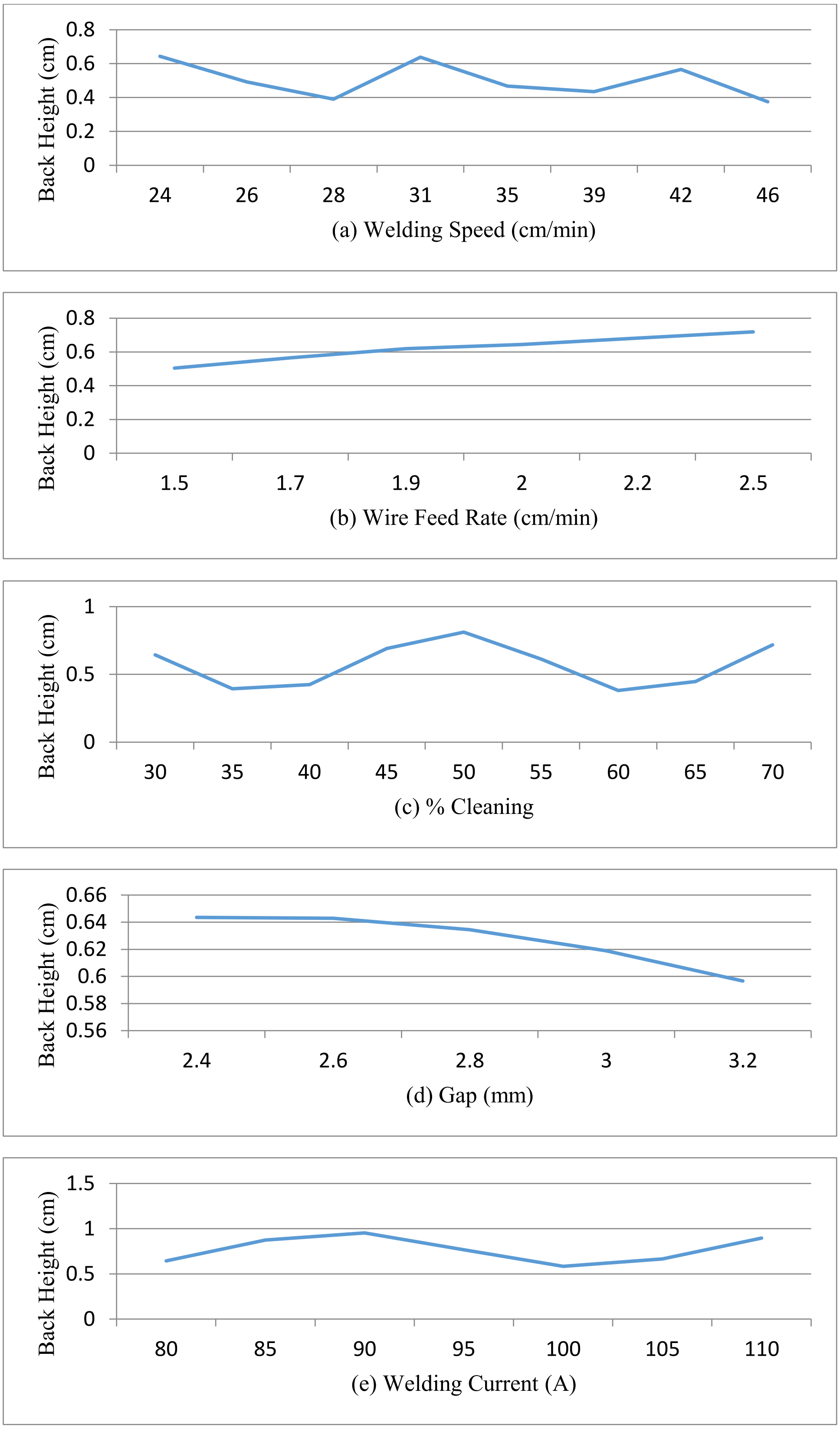

Figure 5.5 Effects of Independent Input Variables on Back Height

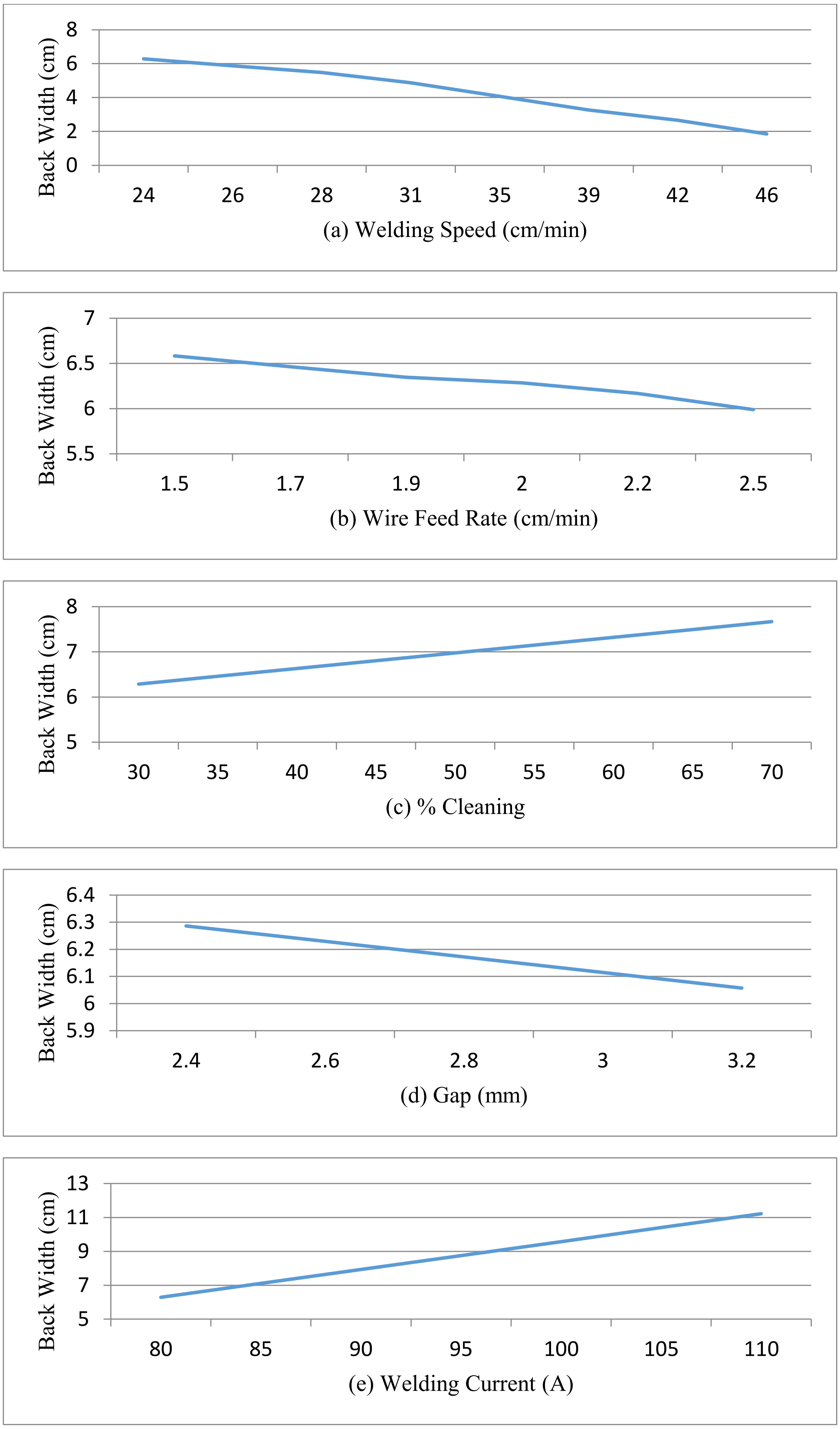

Figure 5.6 Effects of Independent Input Variables on Back Width

5.3. Optimization

The main reason to use hybrid study of regression analysis and ANN instead of conventional regression analysis is to express that conventional regression analysis cannot correspond response variable completely. Based on this comparing, models are selected separately for four response variables by examining R^2 and R^2 testing obtained from hybrid application of regression analysis and ANN. Optimization studies are operated by choosing front width from weld bead geometric dimensions.

Front width needs to be shortest when compared with other three weld bead dimensions. Material absorbs heat as much as width of weld bead. This heat absorption results in distortion. Concurrently, heat absorption and distortion cause weld cracks. TIG welding process is expensive process that it should be considered while selecting objective.

Generated regression model for front width is given in Appendix D. Front width equation in Appendix D is selected by comparing R^2 and R^2 testing. R^2 and R^2 testing should be close to 1.000 and also close to each other. Optimization problems are solved by using selected model which expresses physical problem correctly that is Front width equation in Appendix A. Two different problem with different constraints are examined for front width in this study. These two problems are detailed in Table 5.4. Problem 1 is single objective, nonlinear constraint problem in continuous domain. Problem 2 is also single objective with nonlinear constraint in mixed integer continuous domain. They could not be solved with standard Nelder-Mead or classical optimization approach. Because of the complexity of problems, stochastic optimization methods are used.

Table 5.4 Optimization problems, constraints, input variables, used optimization algorithms

Pro. No	Problem	Constraint	Input Variable	Optimization Algorithm
1	Front Width (FW) Minimization	FW > 0 -1 < FH < 1 0 < BH < 1 1 < BW < 13 24 < Welding Speed < 46 1.5 < Wire Feed Rate < 2.5 30 < % Cleaning < 70 2.4 < Gap < 3.2 80 < Welding Current < 110	Welding Speed (A) Wire Feed Rate (B) % Cleaning (C) Gap (D) Welding Current (E)	Differential Evolution (DE)
2	Front Width (FW) Minimization	FW > 0 -1 < FH < 1 0 < BH < 1 1 < BW < 13 24 < Welding Speed < 46 1.5 < Wire Feed Rate < 2.5 30 < % Cleaning < 70 80 < Welding Current < 110 {2.4, 2.5, 2.6, 2.7, 2.8, 2.9, 3.0, 3.1, 3.2} ∈ Gap Welding Speed ∈ Integer % Cleaning ∈ Integer Welding Current ∈ Integer	Welding Speed (A) Wire Feed Rate (B) % Cleaning (C) Gap (D) Welding Current (E)	Differential Evolution (DE) Nelder Mead (NM) Simulated Annealing(SA) Random Search (RS)

NMinimize tool in Wolfram Mathematica is used to minimize Front Width for problems considered. In the first problem, input parameters welding speed, wire feed rate, percentage of cleaning, gap, welding current, and the response variables front height, back height, and back width are considered as constraints in continuous domain. Front width is also given as constraint which is bigger than zero. Front height could be less than zero physically, which means line of work pieces are considered as zero point. Gap under this line is considered as minus state. Back height could also be less than zero physically. Nevertheless, minimum back height point is taken as zero which means in this thesis. Differential evolution is used as optimization method for this problem because of the characteristic of equation. However, it is impossible to use these input values with precise fractions in fields of industry when problem constraints are selected continuous. Therefore, with the addition to constraints in the first problem, welding speed, % cleaning, and welding current are assumed to be integer for the second problem. Gap between work pieces is constrained as having integer series starting 2.4 mm to 3.2 mm with 0.1 mm increment. Results of Problem 1 indicates better results than the results of Problem 2, although application of constraints for Problem 1 in field is very hard to manufacture. After adding industry constraints which are in-field application limits and using front width model in Appendix D, the optimum results for FW obtained by four different stochastic optimization methods DE, NM, SA, and RS are given in Table 5.5. Comparing the results, it can be concluded that Differential Evolution method should be selected to have minimum front width.

Table 5.5 Minimized Front Width Values by the methods used in this thesis

Method	Minimized FW (cm)	A (cm/min)	B (cm/min)	C (%)	D (mm)	E (A)	Reliability
Problem 1							
DE	3.17041	46	1.5	61.5118	3.2	80	100%
Problem 2							
DE	3.33987	45	1.5	31	2.4	81	100%
NM	3.39013	45	1.5	31	3.2	81	100%
SA	3.44934	45	1.5001	33	2.5	81	100%
RS	3.55867	45	1.5	40	3.2	82	100%

CHAPTER 6

CONCLUSION

In this thesis, geometric dimensions of weld bead in a tungsten inert gas (TIG) welding process is minimized by using stochastic optimization methods which are Differential Evolutions, Nelder Mead, Simulated Annealing, and Random Search. Welding is a complex process that could be affected by several variables. Geometric dimensions of weld bead are important elements for quality of TIG welding process. Quality of welding meets with other requirements in industrial fields like profile of material, positioning, and flatness in TIG welding process. It is also a critical item to have heat, what makes the material distorted and creates weld crack. Distortion of material and crack formation could be decreased having minimum heat affected zone. Weld bead dimensions should be reduced to have minimum heat affected zone. In order to have minimum distortion, optimization of weld bead geometric parameters becomes fundamental.

Weld speed, weld feed rate, gap, cleaning percentage, and welding current are considered as input variables in TIG welding process to take under control. These parameters are indicated as system constraints. Six different mathematical models which are polynomial, polynomial rational, logarithmic, logarithmic rational, trigonometric, trigonometric rational for each four response variables (front height, front width, back height, and back width of weld bead) were examined. TIG welding process modelling is generated with neuro-regression approach in Mathematica software with NMinimize tool. Differential Evolution, Nelder Mead, Simulated Annealing, and Random Search algorithms were used to minimize geometric dimensions of weld bead.

Conventional regression analysis is operated to find coefficient of determination, and coefficient of determination adjusted. Regression analysis and ANN are performed to have substantial model by comparing training and testing coefficients of determination. The aim of this progress is to understand deviation between conventional regression analysis, and neuro-regression analysis. As a result of progress, it is seen that conventional regression analysis could not give reliable result. Third order polynomial model is selected as an objective function to minimize front width by using regression analysis and ANN. Model itself is given as constraint that was bigger than zero to have reasonable result. Welding speed is required to be between 24 and 46 cm/min, wire feed rate is required to be between 1.5 and 2.5 cm/min. Cleaning percentage is asked to be equal or higher than 30 and equal or lower than 70. Gap should be between 2.4 and 3.2 mm and welding current is asked to be between 80 and 110 A.

According to results, it can be concluded that maximum welding speed (45 cm/min), minimum wire feed rate(1.5 cm/min), minimum cleaning percentage (31 %), minimum gap (2.4 mm), and minimum current (81 A), give minimum front width (3.33987 cm), value of weld bead in TIG welding process.

As a future work, heat affected zone (HAZ) optimization can be studied. HAZ is the area around weld bead, which is non-melted area that has changes in its microstructure by heat. Heat affected zone should be minimum in work pieces due to absorb minimum heat. Heat makes work pieces distorted after welding application.

REFERENCES

Singh R., Welding and Joining Processes, Applied Welding Engineering, (2016), 163-195.

Choudhary A., & Kumar M., & Unune D. R., Experimental investigation of weld bead characteristic during submerged arc welding of AISI 1023 steel, Defense Technology, 15 (2018).

Nanda H. K., & Balasubramanian K. R., Parametric Optimization of TIG Welding on 316L Austenitic Stainless Steel by Grey-Based Taguchi Method, Advanced Materials Research, (2011), 383-390.

Yang L. J., & Chandel R. S., & Bibby M. J., An analysis of curvilinear regression equations for modeling the submerged arc welding process, Journal of Material Processing Technology, 37 (1993), 601-611.

Vedrtnam A., & Singh G., & Kumar A., Optimization submerged arc welding using response surface methodology, regression analysis, and genetic algorithm, Defense Technology, (2018).

Murugan N., & Gunaraj V., Prediction and control of weld bead geometry and shape relationships in submerged arc welding of pipes, Journal of Materials Processing Technology, 168 (2005), 478-487.

Lee J. I. & Rhee S., Prediction of process parameters for gas metal arc welding by multiple regression analysis, Proc. of Institution of Mechanical Engineers, 214 (2000), 443-449.

Tarn Y. S., & Juang S. C., & Lii H. R., A comparison between the back-propagation and counter-propagation networks in the modeling of the TIG welding process, Journal of Materials Processing Technology, 75 (1998), 54-62.

Anderson K., & Cook G. E., & Ramaswamy K., Artificial neural network applied to arc welding process modeling and control, IEEE Trans. Indus. Appl., 26 (1990), 824-830.

Dey V., & Pratihar D. K., & Datta G. L. & Jha M. N., & Saha T. K., & Bapat A. V., Optimization and prediction of weldment profile in bead-on-plate welding of A11100 plates using electron beam, Int. J. Adv. Manuf. Tech., 48 (2010), 513-528.

Joby J., & Muthukumaran S., Optimization of activated TIG welding parameters for improving weld joint strength of AISI 4135 PM Steel by genetic algorithm and simulated annealing, Int. J. Adv. Manuf. Tech., Springer-Verlag London, Vol. 6, Issue 72, (2015).

Nagaraju S., & Vasantharaja P., & Chandrasekhar N., & Vasudevan M., & Jayakumar T., Optimization of welding process parameters for 9Cr-1Mo steel using RSM and GA, Mater. Manuf. Process., (2016), 319-327.

Chandrasekhar N., & Ragavendran M., & Ravikumar R., & Vasudevan M., & Murugan S., Optimization of hybrid laser-TIG welding of 316LN stainless steel using genetic algorithm, Mater. Manuf. Process., (2017), 1094-1100.

Weman K., TIG welding, Welding Process Handbook, (2012), 63-69.

Ericsson M., Simulated of robotic TIG-welding, MSC Thesis, Department of Technology University of Trollhattan/Uddevalla, Trollhattan, Sweden, (2003).

Awang M., The effects of process parameters on steel welding response in curved plates, MSC Thesis, College of Engineering and Mineral Resources West Virginia University, Morgantown, West Virginia, (2002).

Muncaster P. W., Basic TIG welding requirements, A Practical Guide to TIG (GTA) Welding, (1991), 15-33.

Mathers G., TIG welding, The Welding of Aluminum and Its Alloys, (2012), 97-115.
Mishra S., & Datta-Gupta A., Regression Modeling and Analysis, Applied Statistical Modeling and Data Analytics, (2018), 69-96.

Pinder J. P., Regression, Introduction to Business Analytics Using Simulation, (2017), 313-369

Kissell R., & Poserina J., Regression Models, Optimal Sports Math, Statistics, and Fantasy, (2017), 39-67.

Aster R. C., & Borchers B., & Thurber C. H., Nonlinear Regression, Parameter Estimation and Inverse Problems, (2019), 235-256

Rao S. S., Stochastic Programming, Engineering Optimization: Theory and Practice, Fourth Edition, (2009), 632-667.

Rao S. S., Classical Optimization Techniques, Engineering Optimization: Theory and Practice, Fourth Edition, (2009), 63-118.

Rao S. S., Introduction to Optimization, Engineering Optimization: Theory and Practice, Fourth Edition, (2009), 1-62.

Yang X., Differential Evolution, Nature-Inspired Optimization Algorithms, (2014), 89-97.

Nelder J. A., & Mead R., A simplex-method for function minimization, Computer Journal, 7(4) (1965), 308 – 313.

Xu S., Wang Y., Wang Z., Parameters estimation of proton exchange membrane fuel cells using Eagle strategy based on JAYA algorithm and Nelder-Mead simplex method, Energy, (2019).

Zabinsky Z. B., Random Search Algorithms, University of Washington, (2009).

Dutta P., & Pratihar D. K., Modeling of TIG welding process using conventional regression analysis and neural network-based approaches, Journal of Materials Processing Technology, 84 (2007), 56-68.

Cortes-Antonio P., & Rangel-Gonzalez J., & Villa-Vargas L. A., & Ramirez-Salinas M., A., & Morina-Lozano H., & Batyrshin I., Design and Implementation of Differential Evolution Algorithm on FPGA for Double-Precision Floating-Point Representation, Acha Polytechnica Hungarica, Vol 11, No. 4, (2014)

Wang L., & Xu Y., & Li L., Parameter identification of chaotic systems by hybrid Nelder-Mead simplex search and dfferential evolution algorithm, Expert Systems with Applications, 38 (2011), 3238-3245.

Shao Q., & Xu T., & Yoshino T., & Song N., Multi-objective optimization of gas metal arc welding parameters and sequences for low-carbon steel (Q345D) T-joints, Journal of Iron and Steel Research International, (2017), 544-555.

Direct Industry, CEBORA welding&cutting http://www.directindustry.com/prod/cebora/product-12065-1220217.html

Bob The Welder, 4.0m WP-18 Water Cooled Power cable 9540V64 https://www.bobthewelder.com.au/4.0m-WP-18-Water-Cooled-Power-cable-9540V64.html

Pham D. & Karaboga D., Intelligent Optimisation Techniques: Genetic Algorithms, Tabu Search, Simulated Annealing and Neural Newtworks. Springer Science & Business Media, (2012)

Karnopp D.C., Random search techniques for optimization problems. Automatica 1 (2-3), 111-121, (1963)

Weisstein, Eric W, “Least Squares Fitting.” From MathWorld—A Wolfram Web

Resources. (2019) http:/matworld.wolfram.com/LeastSquaresFitting.html

Starling C.M.D, Marques P.V. Modenesi P.J., Statistical modelling of narrow-gap GTA welding with magnetic arc oscillation, Journal of Materials Processing Technology, 37-49, (1995)

Koleva E, Statistical modelling and computer programs for optimization of the electron beam welding of stainless steel, Vacuum, 151-157, (2001)

Chan B., Pacey J., Bibbly M., Modelling gas metal arc weld geometry using artificial neural network technology, Canadian Metallurgical Quarterly, 43-51, (1199)

Anawa E.M, Olabi A.G, Optimization of tensile strength of ferritic/austenitic laser-welded components, Optic and Laser in Engineering, 571-577, (2008)

Juang S.C, Tarng Y.S., Process parameter selection for optimizing the weld pool geometry in the tungsten inert gas welding of stainless steel, Journal of Materials Processing Technology, 33-37, (2002)

Bodkhe S.C & Dolas D.R, Optimization of Activated Tungsten Inert Gas Welding of 304L Austenitic Stainless Steel, Procedia Manufacturing 20, 277-282, (2018)

Wei Y., Hua Z., Zhi-gang J., Hon K.K.B., Multi-objective optimization of arc welding parameters – the trade-offs between energy and thermal efficiency, Journal of Cleaner Production, (2016)

Tafarroj M.M & Kolahan F., A comparative study on the performance of artificial neural networks and regression models in modelling the heat source model parameters in GTA welding, Fusion Engineering and Design, 131, 111-118, (2018)

Juang S.C., Tarng Y.S. & Lii H.R., A comparison between the back-propagation and counter-propagation networks in the modeling of the TIG welding process, Journal of Materials Processing Technology, 75, 54-62, (1998)

APPENDIX A

WOLFRAM MATHEMATICA CODE EXAMPLE FOR R-SQUARED CONVENTIONAL, R-SQUARED ADJUSTED, R-SQUARED TRAINING AND R-SQUARED TESTING

```
DATA=
        Table[{A%80[[i]],B%80[[i]],C%80[[i]],D%80[[i]],E%80[[i]],FH%80[[i]]},{i
,1,Length[FW%80]}];
MODEL=
        Expand[(1+Log[0.1 A]+Log[B]+Log[0.1 C]+Log[D]+Log[0.1 E])^1];
CC=Table[a[i],{i,1,Length[MODEL]}];
DD=Table[b[i],{i,1,Length[MODEL]}];
YY=Table[(CC[[i]] MODEL[[i]]),{i,1,Length[MODEL]}]//Total;
ZZ=Table[(DD[[i]]modelnn[[i]]),{i,1,Length[MODEL]}]//Total;
coef={CC,DD}//Flatten;
TT=YY;
constFW=
NonlinearModelFit[DATA,TT,coef,{A,B,C,D,E},MaxIterations→400];
modelFW=constFW//Normal;
constFW[{"RSquared","AdjustedRSquared"}];
constFW[{"PredictedResponse","Response"}]//Transpose//TableForm;
TESTDATA=
        Table[{A%20[[i]],B%20[[i]],C%20[[i]],D%20[[i]],E%20[[i]]},{i,1,Length[A
%20]}];
modelFW/.x1→A%20[[1]]/.x2→B%20[[1]]/.x3→C%20[[1]]/.x4→D%20[[1]]/.x5→
E%20[[1]];
```

(cont.)

FW%20predicted=

Table[modelFW/.x1→A%20[[i]]/.x2→B%20[[i]]/.x3→C%20[[i]]/.x4→ D%20[[i]]/.x5→E%20[[i]],{i,1,Length[A%20]}];

Table[{FW%20[[i]],FW%20predicted[[i]]},{i,1,Length[A%20]}]//TableForm

SSE = Σ (FW%20 – FW%20predicted)^2;

FWbar = Mean[FH%20];

SST = Σ (FW%20 – FWbar)^2

$R^2_{testing}$=1 - SSE/SST

APPENDIX B

R-SQUARED AND R-SQUARED ADJUSTED VALUES FOR OUTPUT VARIABLES WITH SELECTED MODELS

Output	Order	Logarithmic		Log. Rational		Polynomial	
		R^2	R^2 adj	R^2	R^2 adj	R^2	R^2 adj
FH	1th	0.8947	0.84205	0.899186	0.848779	0.891411	0.837116
	2nd	0.904595	2	0.964844	1.21094	0.904917	1.5705
	3rd	0.956384	1.02066	0.965914	1.01615	0.956166	1.02076
	4th	0.980588	1.00324	0.958304	1.00695	0.98002	1.00333
	5th	0.98972	1.00079	0.959147	1.00314	0.989869	1.00078
	6th	1	1	0.96104	1.00158	1	1
FW	1th	0.99145	0.987175	0.99802	0.99703	0.990996	0.986494
	2nd	0.998343	1.00994	0.999399	1.0036	0.998245	1.01053
	3rd	0.999484	1.00024	0.99963	1.00018	0.999505	1.00023
	4th	0.999727	1.00005	0.998739	1.00021	0.999719	1.00005
	5th	0.999962	1	0.998925	1.00008	0.999953	1
	6th	1	1	0.998933	1.00004	1	1
BH	1th	0.976433	0.96465	0.980424	0.970636	0.975797	0.963695
	2nd	0.980574	1.11656	0.995284	1.0283	0.980544	1.11674
	3rd	0.991654	1.00395	0.996278	1.00176	0.991347	1.0041
	4th	0.996795	1.00053	0.99045	1.00159	0.996664	1.00056
	5th	0.999131	1.00007	0.991199	1.00068	0.998986	1.00008
	6th	1	1	0.991234	1.00036	1	1
BW	1th	0.992668	0.989002	0.996088	0.994132	0.99264	0.98896
	2nd	0.997143	1.01714	0.998957	1.00626	0.996985	1.01809
	3rd	0.998574	1.00068	0.998223	1.00084	0.998544	1.00069
	4th	0.999569	1.00007	0.997828	1.00036	0.9996	1.00007
	5th	0.999698	1.00002	0.998523	1.00011	0.99967	1.00003
	6th	1	1	0.998251	1.00007	1	1

(cont.)

Output	Order			Pol. Rational		Trigonometric	
		R^2	R^2 adj	R^2	R^2 adj	R^2	R^2 adj
FH	1th	0.900818	0.851228	0.895455	0.731171	0.567023	-0.11337
	2nd	0.95379	1.27726	0.920826	1.02969	0.969778	1.01133
	3rd	0.964819	1.01666	0.982819	1.00115	0.996712	1.00022
	4th	0.941945	1.00968	1	1	1	1
	5th	0.943566	1.00434	1	1	1	1
	6th	0.952907	1.00191	1	1	1	1
FW	1th	0.998257	0.997386	0.99187	0.979095	0.950009	0.871451
	2nd	0.999363	1.00382	0.999062	1.00035	0.998618	1.00052
	3rd	0.999432	1.00027	0.999783	1.00001	0.999605	1.00003
	4th	0.998582	1.00024	1	1	0.999996	1
	5th	0.9987	1.0001	1	1	0.252416	1.00451
	6th	0.998806	1.00005	1	1	0.237712	1.00172
BH	1th	0.980101	0.970152	0.977491	0.942121	0.973365	0.931511
	2nd	0.977105	1.13737	0.98426	1.0059	0.990641	1.00351
	3rd	0.98014	1.00941	0.998302	1.00011	0.999999	1
	4th	0.988789	1.00187	1	1	1	1
	5th	0.990191	1.00075	1	1	0.681441	1.00192
	6th	0.991097	1.00036	1	1	0.649548	1.00079
BW	1th	0.996601	0.994902	0.992797	0.981479	0.940466	0.846912
	2nd	0.997305	1.01617	0.998206	1.00067	0.995401	1.00172
	3rd	0.997783	1.00105	0.999107	1.00006	0.59714	1.02706
	4th	0.997087	1.00049	1	1	1	1
	5th	0.996953	1.00023	1	1	0.669474	1.00199
	6th	0.997236	1.00011	1	1	0.225343	1.00175

APPENDIX C

R-SQUARED TRAINING AND R-SQUARED TESTING FOR OUTPUT VARIABLES WITH SELECTED MODELS

Output	Order	Logarithmic		Log. Rational		Polynomial	
		R^2	R^2 test	R^2	R^2 test	R^2	R^2 test
FH	1st	0.877253	0.847894	0.897219	0.725835	**0.879363**	**0.858166**
	2nd	0.925005	0.680165	0.990344	-0.176411	0.923898	0.708782
	3rd	0.971589	0.51228	0.987217	0.284667	0.970802	0.48898
	4th	1	-0.065012	0.973244	0.575431	1	-0.418427
	5th	1	-0.0204018	0.974824	0.569497	1	-0.296202
	6th	1	0.0205316	0.976919	0.467487	1	-0.195185
FW	1st	0.992565	0.850227	0.998866	0.586021	0.992038	0.845461
	2nd	0.99925	0.852513	0.999733	0.638972	0.999154	0.843342
	3rd	0.999823	0.887981	0.999873	0.776223	**0.999817**	**0.893814**
	4th	1	0.620821	0.999349	0.617283	1	0.791983
	5th	1	0.679303	0.999545	0.631521	1	0.829917
	6th	1	0.726016	0.999537	0.710238	1	0.856988
BH	1st	0.97582	0.766135	0.984356	-37.5549	0.975162	0.761649
	2nd	0.985547	0.259986	0.996637	-2.69596	0.985305	0.350216
	3rd	0.995368	-0.518445	0.997399	0.164532	0.995196	-0.809078
	4th	1	-0.833585	0.99576	-0.548533	1	-0.792721
	5th	1	-0.705818	0.995966	-0.369399	1	-0.723772
	6th	1	-0.611025	0.99606	-0.598466	1	-0.671118
BW	1st	0.992327	0.956798	0.996814	0.763449	**0.992247**	**0.957525**
	2nd	0.99738	0.894231	0.997962	0.696911	0.997644	0.885322
	3rd	0.999607	0.920849	0.998797	0.715577	0.999573	0.923685
	4th	1	0.561736	0.998257	0.708259	1	0.650419
	5th	1	0.618192	0.998613	0.775196	1	0.699383
	6th	1	0.663795	0.99871	0.738756	1	0.735914

(cont.)

Output	Order		Pol. Rational		Trigonometric	Tri. Rational
		R^2	R^2 test	R^2	R^2 test	R^2	R^2 test
FH	1st	0.900158	0.737413	0.880375	0.848579	0.902199	0.744121
	2nd	0.971561	-13.1967	0.961813	0.54476	0.998113	-8.40019
	3rd	0.984621	-54.5618	1	0.296255	1	0.099373
	4th	0.96718	-3.77035	1	0.638312	1	0.321565
	5th	0.972776	-1.25472	1	0.643954	1	0.773405
	6th	0.974074	-3.4743	1	0.593425	1	0.638154
FW	1st	0.999056	0.682254	0.992828	0.861457	0.999166	0.707001
	2nd	0.999514	0.745395	0.999761	0.871216	0.999917	-0.746051
	3rd	0.999706	0.780684	1	0.893519	0.998609	-218.623
	4th	0.999443	0.6826	1	0.765666	0.999159	-15.8174
	5th	0.999512	0.690136	1	0.578588	0.724865	-13.9773
	6th	0.999551	0.708321	1	0.377448	0.787355	-11.7098
BH	1st	0.983975	-16.7888	**0.976076**	**0.785766**	0.98194	-3983.05
	2nd	0.977283	0.752807	0.990012	-0.12792	0.998532	0.222698
	3rd	0.97829	0.774019	1	0.00500573	0.999999	-35.2269
	4th	0.993415	-1.10966	1	0.625901	1	-263.313
	5th	0.99398	-4.79706	1	0.562069	1	-3.85913
	6th	0.993947	-1.74982	1	0.409722	1	-0.91696
BW	1st	0.997298	0.797323	0.992492	0.95577	0.998193	0.631543
	2nd	0.997861	0.559927	0.999093	0.936805	0.99928	0.78918
	3rd	0.99818	0.55255	1	0.802684	0.78549	-5.16891
	4th	0.997597	0.687815	1	0.819147	0.999452	-626.84
	5th	0.9978	0.425155	1	0.736966	0.764177	-5.69487
	6th	0.997965	0.489424	1	0.631493	0.99072	-7.94175

APPENDIX D

MODELS FOR FRONT HEIGHT, FRONT WIDTH, BACK HEIGHT, AND BACK WIDTH

$$
\mathbf{FRONTHEIGHT} = 0.568524101629537 + 0.00971854565928604\mathbf{A} + 0.28426205081476735\mathbf{B} - 0.0030044984281893663\mathbf{C} + 0.03350880331253237\mathbf{D} - 0.01639362439199862\mathbf{E};
$$

$$
\mathbf{FRONTWIDTH} = -6.361624897213393 + 0.39356692192362347\mathbf{A} + 0.004420394016303833\mathbf{A}^2 - 0.00029169434635837173\mathbf{A}^3 - 3.1808124486072673\mathbf{B} + 0.19678346096190014\mathbf{AB} + 0.00221019700815087\mathbf{A^2B} - 1.5904062243036705\mathbf{B^2} + 0.09839173048089371\mathbf{AB^2} - 0.7952031121519639\mathbf{B^3} - 0.006436711715044893\mathbf{C} + 0.0007811167929886863\mathbf{AC} + 0.00010382598234901175\mathbf{A^2C} - 0.003218355857552146\mathbf{BC} + 0.00039055839649413835\mathbf{ABC} - 0.001609177928767246 5\mathbf{B^2C} + 0.0008611815046496747\mathbf{C^2} - 0.000041283641234907 49\mathbf{AC^2} + 0.0004305907523248826\mathbf{BC^2} + 0.000018641477159669774\mathbf{C^3} - 1.316325687111202\mathbf{D} - 0.008551412859786101\mathbf{AD} + 0.0018699372073450 93\mathbf{A^2D} - 0.6581628435555597\mathbf{BD} - 0.004275706429892794\mathbf{ABD} - 0.3290814217777845\mathbf{B^2D} + 0.00935551932978515\mathbf{CD} - 0.0007722065630192928\mathbf{ACD} + 0.004677759664892573\mathbf{BCD} + 0.00042852282617298547\mathbf{C^2D} - 0.14654394780458987\mathbf{D^2} - 0.04877480090938328 4\mathbf{AD^2} - 0.07327197390229494\mathbf{BD^2} + 0.006876836086975487\mathbf{CD^2} + 0.03832252844444908\mathbf{D^3} + 0.13215108851236587\mathbf{E} - 0.014364160271117987\mathbf{AE} + 0.00016059340137669054\mathbf{A^2E} + 0.06607554425618294\mathbf{BE} - 0.007182080135558993\mathbf{ABE} + 0.03303777212809147\mathbf{B^2E} - 0.0011877721082901053\mathbf{CE} - 0.00004121995411029513\mathbf{ACE} - 0.0005938860541450527\mathbf{BCE} - 0.00004879662379406077\mathbf{C^2E} + 0.04760878000890453\mathbf{DE} + 0.0018987479230951662\mathbf{ADE} + 0.02380439000445226 7\mathbf{BDE} - 0.0008345086306933741\mathbf{CDE} + 0.016187091515234155\mathbf{D^2E} + 0.0010968086690896 11\mathbf{E^2} + 0.000039693277421732845\mathbf{AE^2} + 0.0005484043345448055\mathbf{BE^2} + 0.000062961473745288 17\mathbf{CE^2} - 0.0010880809399478 86\mathbf{DE^2} - 0.0000113285698922002 3\mathbf{E^3};
$$

$$
\mathbf{BACKHEIGHT} = 0.12968678075332998 + 0.09500624332313756\mathrm{Cos}[\mathbf{A}] - 0.31163706981258893\mathrm{Cos}[\mathbf{B}] + 0.22488483665678763\mathrm{Cos}[\mathbf{C}] - 0.15208658410885711\mathrm{Cos}[\mathbf{D}] - 0.1322623876221588\mathrm{Cos}[\mathbf{E}] - 0.10334728042952393\mathrm{Sin}[\mathbf{A}] + 0.1426230592184351\mathrm{Sin}[\mathbf{B}] - 0.01918842077475885\mathrm{Sin}[\mathbf{C}] + 0.11799472705967291\mathrm{Sin}[\mathbf{D}] + 0.14038093336277016\mathrm{Sin}[\mathbf{E}];
$$

$$
\mathbf{BACKWIDTH} = -1.1889712127077077 - 0.20140903545851221\mathbf{A} - 0.5944856063538464\mathbf{B} + 0.034565009032046186\mathbf{C} - 0.2864699361891838\mathbf{D} + 0.16435728272259495\mathbf{E};
$$